

1
2 **Mitochondrial respiratory states and rates:**
3 **Building blocks of mitochondrial physiology Part 1**
4

5 **COST Action CA15203 MitoEAGLE preprint** Version: 2018-09-04(41)

6 Corresponding author: Gnaiger E

7 Co-authors:

8 Aasander Frostner E, Abumrad NA, Acuna-Castroviejo D, Ahn B, Ali SS, Alves MG, Amati
9 F, Amoedo ND, Aral C, Arandarçikaitè O, Bailey DM, Bajpeyi S, Bakker BM, Bastos
10 Sant'Anna Silva AC, Battino M, Bazil J, Beard DA, Bednarczyk P, Ben-Shachar D, Bergdahl
11 A, Bernardi P, Bishop D, Blier PU, Boetker HE, Boros M, Borsheim E, Borutaitè V,
12 Bouillaud F, Bouitbir J, Breton S, Brown DA, Brown GC, Brown RA, Brozinick JT, Buettner
13 GR, Burtcher J, Calabria E, Calbet JA, Calzia E, Cannon DT, Canto AC, Cardoso LHD,
14 Carvalho E, Casado Pinna M, Cassina AM, Castro L, Cavalcanti-de-Albuquerque JP,
15 Cervinkova Z, Chaurasia B, Chen Q, Chicco AJ, Chinopoulos C, Chowdhury SK, Clementi E,
16 Coen PM, Coker RH, Collin A, Crisóstomo L, Di Marcello M, Darveau CA, Das AM, Dash
17 RK, Davis MS, De Palma C, Dembinska-Kiec A, Dias TR, Distefano G, Doerrier C, Drahota
18 Z, Dubouchaud H, Duchen MR, Dumas JF, Durham WJ, Dymkowska D, Dyrstad SE,
19 Dzialowski EM, Ehinger J, Elmer E, Endlicher R, Engin AB, Fell DA, Ferko M, Ferreira
20 JCB, Ferreira R, Fessel JP, Filipovska A, Fisar Z, Fischer M, Fisher G, Fisher JJ, Fornaro M,
21 Galina A, Galkin A, Gan Z, Garcia-Roves PM, Garcia-Souza LF, Garipi E, Garlid KD,
22 Garrabou G, Garten A, Gastaldelli A, Genova ML, Giovarelli M, Gonzalez-Armenta JL,
23 Gonzalo H, Goodpaster BH, Gorr TA, Gourlay CW, Granata C, Grefte S, Gueguen N, Haas
24 CB, Haavik J, Haendeler J, Hamann A, Han J, Hancock CR, Hand SC, Hargreaves IP,
25 Harrison DK, Heales SJR, Hellgren KT, Hepple RT, Hernansanz-Agustin P, Hickey AJ, Hoel
26 F, Holland OJ, Holloway GP, Hoppel CL, Houstek J, Hunger M, Iglesias-Gonzalez J, Irving
27 BA, Iyer S, Jackson CB, Jadiya P, Jang DH, Jang YC, Jansen-Dürr P, Jarmuszkiewicz W,
28 Jespersen NR, Jha RK, Jurk D, Kaambre T, Kaczor JJ, Kainulainen H, Kandel SM, Kane DA,
29 Kappler L, Karabatsiakos A, Karkucinska-Wieckowska A, Keijer J, Keppner G, Khamoui AV,
30 Klingenspor M, Komlodi T, Koopman WJH, Kopitar-Jerala N, Kowaltowski AJ, Kozlov AV,
31 Krajcova A, Krako Jakovljevic N, Kristal BS, Kuang J, Kucera O, Kwak HB, Kwast K,
32 Labieniec-Watala M, Lai N, Land JM, Lane N, Laner V, Lanza IR, Larsen TS, Lavery GG,
33 Lee HK, Leuwenburgh C, Lemieux H, Lerfall J, Li PA, Liu J, Lucchinetti E, Macedo MP,
34 MacMillan-Crow LA, Makrecka-Kuka M, Malik A, Markova M, Martin DS, Mazat JP,
35 McKenna HT, Menze MA, Meszaros AT, Methner A, Michalak S, Moellering DR, Moiso N,
36 Molina AJA, Montaigne D, Moore AL, Moreau K, Moreno-Sánchez R, Moreira BP, Mracek
37 T, Muntane J, Muntean DM, Murray AJ, Nair KS, Nemeč M, Neuffer PD, Neuzil J, Newsom
38 S, Nozickova K, O'Brien KA, O'Gorman D, Oliveira MF, Oliveira MT, Oliveira PF, Oliveira
39 PJ, Orynbayeva Z, Osiewacz HD, Pak YK, Pallotta ML, Palmeira CM, Parajuli N, Passos JF,
40 Patel HH, Pecina P, Pelnen D, Pereira da Silva Grilo da Silva F, Perez Valencia JA, Pesta D,
41 Petit PX, Pettersen IKN, Pichaud N, Piel S, Pietka TA, Pino MF, Pirkmajer S, Porter C, Porter
42 RK, Pranger F, Prochownik EV, Pulinilkunnit T, Puskarich MA, Puurand M, Quijano C,
43 Radenkovic F, Radi R, Ramzan R, Rattan S, Reboredo P, Rich PR, Renner-Sattler K, Rial E,
44 Robinson MM, Roden M, Rodríguez-Enriquez S, Rohlena J, Rolo AP, Ropelle ER, Røslund
45 GV, Rossignol R, Rossiter HB, Rybacka-Mossakowska J, Saada A, Safaei Z, Salin K,

46 Salvadego D, Sandi C, Sanz A, Sazanov LA, Scatena R, Schartner M, Scheibye-Knudsen M,
 47 Schilling JM, Schlattner U, Schönfeld P, Schwarzer C, Scott GR, Shabalina IG, Sharma P,
 48 Sharma V, Shevchuk I, Siewiera K, Silber AM, Silva AM, Sims CA, Singer D, Skolik R,
 49 Smenes BT, Smith J, Soares FAA, Sobotka O, Sokolova I, Sonkar VK, Sowton AP, Sparagna
 50 GC, Sparks LM, Spinazzi M, Stankova P, Stary C, Stiban J, Stier A, Stocker R, Sumbalova Z,
 51 Suravajhala P, Swerdlow RH, Swiniuch D, Szabo I, Szewczyk A, Szibor M, Tanaka M,
 52 Tandler B, Tarnopolsky MA, Tavernarakis N, Tepp K, Thyfault JP, Tomar D, Towheed A,
 53 Tretter L, Trifunovic A, Trivigno C, Tronstad KJ, Trougakos IP, Tyrrell DJ, Urban T,
 54 Valentine JM, Velika B, Vendelin M, Vercesi AE, Victor VM, Vieyra A Villena JA,
 55 Vinogradov AD, Viscomi C, Vitorino RMP, Vogt S, Volani C, Votion DM, Vujacic-Mirski
 56 K, Wagner BA, Ward ML, Warnsmann V, Wasserman DH, Watala C, Wei YH, Wieckowski
 57 MR, Williams C, Wohlgemuth SE, Wohlwend M, Wolff J, Wüst RCI, Yokota T, Zablocki K,
 58 Zaugg K, Zaugg M, Zhang Y, Zhang YZ, Zischka H, Zorzano A
 59

60 Updates and discussion:

61 http://www.mitoeagle.org/index.php/MitoEAGLE_preprint_2018-02-08

62 Correspondence: Gnaiger E

63 *Chair COST Action CA15203 MitoEAGLE* – <http://www.mitoeagle.org>

64 *Department of Visceral, Transplant and Thoracic Surgery, D. Swarovski Research*
 65 *Laboratory, Medical University of Innsbruck, Innrain 66/4, A-6020 Innsbruck, Austria*

66 *Email: mitoeagle@i-med.ac.at; Tel: +43 512 566796, Fax: +43 512 566796 20*
 67

68 Abstract - Executive summary

69 **1. Introduction** – Box 1: In brief: Mitochondria and Bioblasts

70 **2. Coupling states and rates in mitochondrial preparations**

71 Mitochondrial preparations

72 *2.1. Respiratory control and coupling*

73 The steady-state

74 Specification of biochemical dose

75 Phosphorylation, P_{\gg} , and P_{\gg}/O_2 ratio

76 Control and regulation

77 Respiratory control and response

78 Respiratory coupling control and ET-pathway control

79 Coupling

80 Uncoupling

81 *2.2. Coupling states and respiratory rates*

82 Respiratory capacities in coupling control states

83 LEAK, OXPHOS, ET, ROX

84 *2.3. Classical terminology for isolated mitochondria*

85 States 1–5

86 **3. What is a rate?** – Box 2: Metabolic flows and fluxes: vectorial, vectorial, and scalar

87 **4. Normalization of rate per sample**

88 *4.1. Flow: per object*

89 *4.2. Size-specific flux: per sample size*

90 *4.3. Marker-specific flux: per mitochondrial content*

91 **5. Normalization of rate per system**

92 *5.1. Flow: per chamber*

93 *5.2. Flux: per chamber volume*

94 **6. Conversion of units**

95 **7. Conclusions** – Box 3: Recommendations for studies with mitochondrial preparations

96 **References**

97

98 **Abstract** As the knowledge base and importance of mitochondrial physiology to human health
 99 expands, the necessity for harmonizing the terminology concerning mitochondrial respiratory
 100 states and rates has become increasingly apparent. The chemiosmotic theory establishes the
 101 mechanism of energy transformation and coupling in oxidative phosphorylation. The unifying
 102 concept of the protonmotive force provides the framework for developing a consistent
 103 theoretical foundation of mitochondrial physiology and bioenergetics. We follow IUPAC
 104 guidelines on terminology in physical chemistry, extended by considerations on open systems
 105 and thermodynamics of irreversible processes. The concept-driven constructive terminology
 106 incorporates the meaning of each quantity and aligns concepts and symbols to the nomenclature
 107 of classical bioenergetics. We endeavour to provide a balanced view on mitochondrial
 108 respiratory control and a critical discussion on reporting data of mitochondrial respiration in
 109 terms of metabolic flows and fluxes. Uniform standards for evaluation of respiratory states and
 110 rates will ultimately support the development of databases of mitochondrial respiratory function
 111 in species, tissues, and cells. Clarity of concept and consistency of nomenclature facilitate
 112 effective transdisciplinary communication, education, and ultimately further discovery.

113
 114 *Keywords:* Mitochondrial respiratory control, coupling control, mitochondrial
 115 preparations, protonmotive force, uncoupling, oxidative phosphorylation, OXPHOS,
 116 efficiency, electron transfer, ET; proton leak, LEAK, residual oxygen consumption, ROX, State
 117 2, State 3, State 4, normalization, flow, flux, O₂

119 **Executive summary**

120
 121 In view of the broad implications for health care, mitochondrial researchers face an
 122 increasing responsibility to disseminate their fundamental knowledge and novel discoveries to
 123 a wide range of stakeholders and scientists beyond the group of specialists. This requires
 124 implementation of a commonly accepted terminology within the discipline and standardization
 125 in the translational context. Authors, reviewers, journal editors, and lecturers are challenged to
 126 collaborate with the aim to harmonize the nomenclature in the growing field of mitochondrial
 127 physiology and bioenergetics, from evolutionary biology and comparative physiology to
 128 mitochondrial medicine. In the present communication we focus on the following aspects of
 129 mitochondrial physiology:

- 130 1. Aerobic respiration depends on the coupling of phosphorylation (ADP → ATP) to O₂
 131 flux in catabolic reactions. Coupling in oxidative phosphorylation is mediated by
 132 translocation of protons across the inner mitochondrial membrane through proton
 133 pumps generating or utilizing the protonmotive force, that is measured between the
 134 mitochondrial matrix and intermembrane compartment or outer mitochondrial
 135 space. Compartmental coupling distinguishes vectorial oxidative phosphorylation
 136 from glycolytic fermentation as the counterpart of cellular core energy metabolism
 137 (**Figure 1**). Cell respiration is distinguished from fermentation by: (1) Electron
 138 acceptors supplied by external respiration for the maintenance of redox balance,
 139 whereas fermentation is characterized by an internal electron acceptor produced in
 140 intermediary metabolism. In aerobic cell respiration, redox balance is maintained
 141 by O₂ as the electron acceptor. (2) Compartmental coupling in vectorial oxidative
 142 phosphorylation, in contrast to exclusively scalar substrate-level phosphorylation
 143 in fermentation.
- 144 2. To exclude fermentation and other cytosolic interactions from exerting an effect on the
 145 analysis of mitochondrial metabolism, the barrier function of the plasma membrane
 146 must be disrupted. Selective removal or permeabilization of the plasma membrane
 147 yields mitochondrial preparations—including isolated mitochondria, tissue and
 148 cellular preparations—with structural and functional integrity. Then extra-
 149 mitochondrial concentrations of fuel substrates, ADP, ATP, inorganic phosphate,

and cations including H^+ can be controlled to determine mitochondrial function under a set of conditions defined as coupling control states. A concept-driven terminology of bioenergetics explicitly incorporates in its terms and symbols information on the nature of respiratory states that makes the technical terms readily recognized and easier to understand.

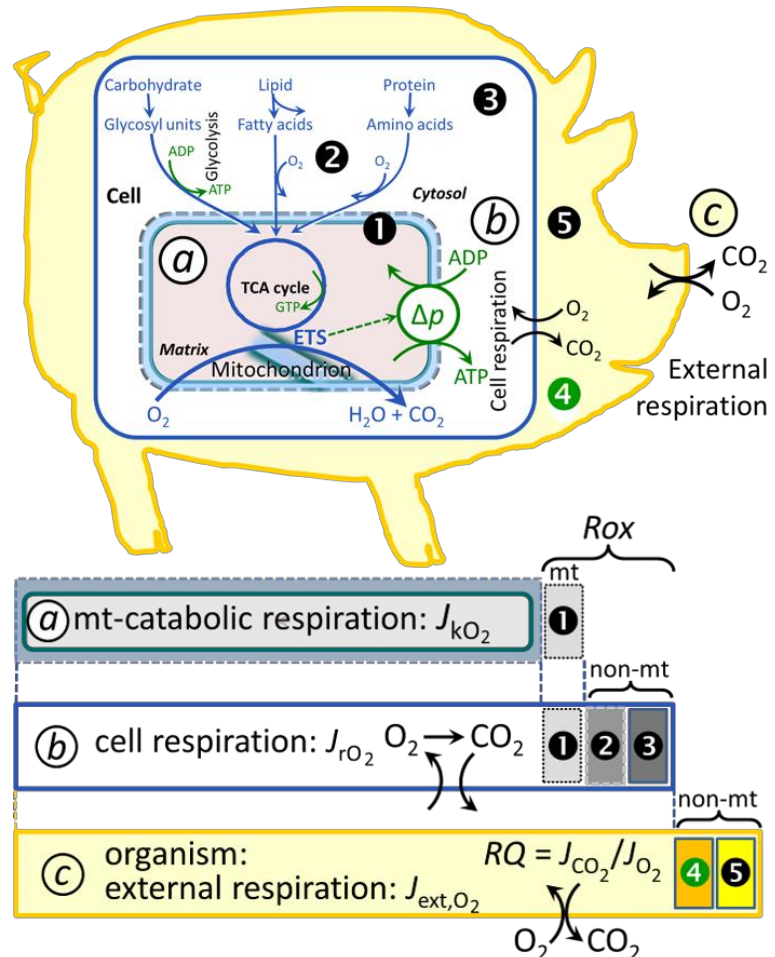
Figure 1. Mitochondrial respiration is the oxidation of fuel substrates (electron donors) and reduction of O_2 catalysed by the electron transfer system, ETS: (a) mitochondrial catabolic respiration; (b) total cellular O_2 consumption; and (c) external respiration

All chemical reactions, r , that consume O_2 in the cells of an organism, contribute to cell respiration, J_{rO_2} . **1** Mitochondrial residual oxygen consumption, Rox . **2** Non-mitochondrial O_2 consumption by catabolic reactions, particularly peroxisomal oxidases and microsomal cytochrome P450 systems. **3** Non-mitochondrial Rox by reactions unrelated to catabolism. $mt-Rox$ and non- $mt Rox$ are measured without fuel substrate supply or after inhibiting the ETS. **4** Aerobic microbial respiration. **5** Extracellular O_2 consumption. Bars are not at a quantitative scale.

a Mitochondrial catabolic respiration, J_{kO_2} , is the O_2 consumption by the mitochondrial ETS excluding Rox .

b Cell respiration, J_{rO_2} , takes into account internal O_2 -consuming reactions, r , including catabolic respiration and Rox . Catabolic cell respiration is the O_2 consumption associated with catabolic pathways in the cell, including mitochondrial catabolism in addition to peroxisomal and microsomal oxidation reactions (**2**).

c External respiration balances internal respiration at steady-state, including aerobic respiration by the microbiome (**4**) and extracellular O_2 consumption (**5**). O_2 is transported from the environment across the respiratory cascade, *i.e.*, circulation between tissues and diffusion across cell membranes, to the intracellular compartment. The respiratory quotient, RQ , is the molar CO_2/O_2 exchange ratio; when combined with the respiratory nitrogen quotient, N/O_2 (mol N given off per mol O_2 consumed), the RQ reflects the proportion of carbohydrate, lipid and protein utilized in cell respiration during aerobically balanced steady-states. Bicarbonate and CO_2 are transported in reverse to the extracellular milieu and the organismic environment. Hemoglobin provides the molecular paradigm for the combination of O_2 and CO_2 exchange, as do lungs and gills on the morphological level.



- 200 3. Mitochondrial coupling states are defined according to the control of respiratory oxygen
 201 flux by the protonmotive force. Capacities of oxidative phosphorylation and
 202 electron transfer are measured at kinetically saturating concentrations of fuel
 203 substrates, ADP and inorganic phosphate, and O₂, or at optimal uncoupler
 204 concentrations, respectively, in the absence of Complex IV inhibitors such as NO,
 205 CO, or H₂S. Respiratory capacity is a measure of the upper bound of the rate of
 206 respiration, depends on the substrate type undergoing oxidation, and provides
 207 reference values for the diagnosis of health and disease, and for evaluation of the
 208 effects of Evolutionary background, Age, Gender and sex, Lifestyle and
 209 Environment.
- 210 4. Incomplete tightness of coupling, *i.e.*, some degree of uncoupling relative to the
 211 substrate-dependent coupling stoichiometry, is a characteristic of energy-
 212 transformations across membranes. Uncoupling is caused by a variety of
 213 physiological, pathological, toxicological, pharmacological and environmental
 214 conditions that exert an influence not only on the proton leak and cation cycling,
 215 but also on proton slip within the proton pumps and the structural integrity of the
 216 mitochondria. A more loosely coupled state is induced by stimulation of
 217 mitochondrial superoxide formation and the bypass of proton pumps. In addition,
 218 uncoupling by application of protonophores represents an experimental
 219 intervention for the transition from a well-coupled to the noncoupled state of
 220 mitochondrial respiration.
- 221 5. Respiratory oxygen consumption rates have to be carefully normalized to enable meta-
 222 analytic studies beyond the question of a particular experiment. Therefore, all raw
 223 data should be published in a supplemental table or open access data repository.
 224 Sample-specific normalization of rates for: (1) the number of objects (cells,
 225 organisms); (2) the volume or mass of the experimental sample; and (3) the
 226 concentration of mitochondrial markers in the experimental chamber is
 227 distinguished from system-specific normalization for the volume of the chamber
 228 (the measuring system).
- 229 6. The consistent use of terms and symbols will facilitate transdisciplinary communication
 230 and support further developments of a database on bioenergetics and mitochondrial
 231 physiology. The present considerations are focused on studies with mitochondrial
 232 preparations. These will be extended in a series of reports on pathway control of
 233 mitochondrial respiration, respiratory states in intact cells, and harmonization of
 234 experimental procedures.

238 **Box 1: In brief – Mitochondria and Bioblasts**

239 *‘For the physiologist, mitochondria afforded the first opportunity for an*
 240 *experimental approach to structure-function relationships, in particular those*
 241 *involved in active transport, vectorial metabolism, and metabolic control*
 242 *mechanisms on a subcellular level’ (Ernster and Schatz 1981).*

243 **Mitochondria** are the oxygen-consuming electrochemical generators evolved from
 244 endosymbiotic bacteria (Margulis 1970; Lane 2005). They were described by Richard Altmann
 245 (1894) as ‘bioblasts’, which include not only the mitochondria as presently defined, but also
 246 symbiotic and free-living bacteria. The word ‘mitochondria’ (Greek mitos: thread; chondros:
 247 granule) was introduced by Carl Benda (1898).

248 Mitochondria form dynamic networks within eukaryotic cells and are morphologically
 249 enclosed by a double membrane. The mitochondrial inner membrane (mtIM) shows dynamic
 250 tubular to disk-shaped cristae that separate the mitochondrial matrix, *i.e.*, the negatively charged
 251 internal mitochondrial compartment, from the intermembrane space; the latter being enclosed

252 by the mitochondrial outer membrane (mtOM) and positively charged with respect to the
253 matrix. The mtIM contains the non-bilayer phospholipid cardiolipin, which is not present in
254 any other eukaryotic cellular membrane. Cardiolipin stabilizes and promotes the formation of
255 respiratory supercomplexes (SC I_nIII_nIV_n), which are supramolecular assemblies based upon
256 specific, though dynamic interactions between individual respiratory complexes (Greggio *et al.*
257 2017; Lenaz *et al.* 2017). Membrane fluidity exerts an influence on functional properties of
258 proteins incorporated in the membranes (Waczulikova *et al.* 2007). In addition to mitochondrial
259 movement along microtubules, mitochondrial morphology can change in response to energy
260 requirements of the cell via processes known as fusion and fission, through which mitochondria
261 communicate within a network (Chan 2006). Intracellular stress factors may cause shrinking or
262 swelling of the mitochondrial matrix, that can ultimately result in permeability transition.

263 Mitochondria are the structural and functional elementary components of cell respiration.
264 Mitochondrial respiration is the reduction of molecular oxygen by electron transfer coupled to
265 electrochemical proton translocation across the mtIM. In the process of oxidative
266 phosphorylation (OXPHOS), the catabolic reaction of oxygen consumption is
267 electrochemically coupled to the transformation of energy in the form of adenosine triphosphate
268 (ATP; Mitchell 1961, 2011). Mitochondria are the powerhouses of the cell which contain the
269 machinery of the OXPHOS-pathways, including transmembrane respiratory complexes (proton
270 pumps with FMN, Fe-S and cytochrome *b*, *c*, *aa*₃ redox systems); alternative dehydrogenases
271 and oxidases; the coenzyme ubiquinone (Q); F-ATPase or ATP synthase; the enzymes of the
272 tricarboxylic acid cycle, fatty acid and amino acid oxidation; transporters of ions, metabolites
273 and co-factors; iron/sulphur cluster synthesis; and mitochondrial kinases related to energy
274 transfer pathways. The mitochondrial proteome comprises over 1,200 proteins (Calvo *et al.*
275 2015; 2017), mostly encoded by nuclear DNA (nDNA), with a variety of functions, many of
276 which are relatively well known (*e.g.*, proteins regulating mitochondrial biogenesis or
277 apoptosis), while others are still under investigation, or need to be identified (*e.g.*, alanine
278 transporter). Only recently has it been possible to use the mammalian mitochondrial proteome
279 to discover and characterize the genetic basis of mitochondrial diseases (Williams *et al.* 2016;
280 Palmfeldt and Bross 2017).

281 Mitochondria can traverse cell boundaries in a process known as horizontal mitochondrial
282 transfer (Torralba *et al.* 2016). There is a constant crosstalk between mitochondria and the other
283 cellular components. The crosstalk between mitochondria and endoplasmic reticulum is
284 involved in the regulation of calcium homeostasis, cell division, autophagy, differentiation, and
285 anti-viral signaling (Murley and Nunnari 2016). Mitochondria contribute to the formation of
286 peroxisomes, which are hybrids of mitochondrial and ER-derived precursors (Sugiura *et al.*
287 2017). Cellular mitochondrial homeostasis (mitostasis) is maintained through regulation at
288 transcriptional, post-translational and epigenetic levels. Cell signalling modules contribute to
289 homeostatic regulation throughout the cell cycle or even cell death by activating proteostatic
290 modules (*e.g.*, the ubiquitin-proteasome and autophagy-lysosome/vacuole pathways; specific
291 proteases like LON) and genome stability modules in response to varying energy demands and
292 stress cues (Quiros *et al.* 2016). Acetylation is a post-translational modification capable of
293 influencing the bioenergetic response, with clinically significant implications for health and
294 disease (Carrico *et al.* 2018).

295 Mitochondria typically maintain several copies of their own circular genome known as
296 mitochondrial DNA (mtDNA; hundred to thousands per cell; Cummins 1998), which is
297 maternally inherited in humans. Biparental mitochondrial inheritance is documented in
298 mammals, birds, fish, reptiles and invertebrate groups, and is even the norm in some bivalve
299 taxonomic groups (Breton *et al.* 2007; White *et al.* 2008). The mitochondrial genome of the
300 angiosperm *Amborella* contains a record of six mitochondrial genome equivalents acquired by
301 horizontal transfer of entire genomes, two from angiosperms, three from algae and one from
302 mosses (Rice *et al.* 2016). However, some organisms such as *Cryptosporidium* species have

303 morphologically and functionally reduced mitochondria without DNA (Liu *et al.* 2016). In
 304 vertebrates but not all invertebrates, mtDNA is compact (16.5 kB in humans) and encodes 13
 305 protein subunits of the transmembrane respiratory Complexes CI, CIII, CIV and F-ATPase, 22
 306 tRNAs, and two RNAs. Additional gene content has been suggested to include microRNAs,
 307 piRNA, smithRNAs, repeat associated RNA, and even additional proteins (Duarte *et al.* 2014;
 308 Lee *et al.* 2015; Cobb *et al.* 2016). The mitochondrial genome requires nuclear-encoded
 309 mitochondrially targeted proteins, *e.g.*, TFAM, for its maintenance and expression (Rackham
 310 *et al.* 2012). Both genomes encode peptides of the membrane spanning redox pumps (CI, CIII
 311 and CIV) and F-ATPase, leading to strong constraints in the coevolution of both genomes (Blier
 312 *et al.* 2001).

313 Mitochondrial dysfunction is associated with a wide variety of genetic and degenerative
 314 diseases. Robust mitochondrial function is supported by physical exercise and caloric balance,
 315 and is central for sustained metabolic health throughout life. Therefore, a more consistent
 316 presentation of mitochondrial physiology will improve our understanding of the etiology of
 317 disease, the diagnostic repertoire of mitochondrial medicine, with a focus on protective
 318 medicine, lifestyle and healthy aging.

319 Abbreviation: mt, as generally used in mtDNA. Mitochondrion is singular and
 320 mitochondria is plural.

321

322

323 1. Introduction

324

325 Mitochondria are the powerhouses of the cell with numerous physiological, molecular,
 326 and genetic functions (**Box 1**). Every study of mitochondrial health and disease is faced with
 327 Evolution, Age, Gender and sex, Lifestyle, and Environment (MitoEAGLE) as essential
 328 background conditions intrinsic to the individual person or cohort, species, tissue and to some
 329 extent even cell line. As a large and coordinated group of laboratories and researchers, the
 330 mission of the global MitoEAGLE Network is to generate the necessary scale, type, and quality
 331 of consistent data sets and conditions to address this intrinsic complexity. Harmonization of
 332 experimental protocols and implementation of a quality control and data management system
 333 are required to interrelate results gathered across a spectrum of studies and to generate a
 334 rigorously monitored database focused on mitochondrial respiratory function. In this way,
 335 researchers from a variety of disciplines can compare their findings using clearly defined and
 336 accepted international standards.

337 Reliability and comparability of quantitative results depend on the accuracy of
 338 measurements under strictly-defined conditions. A conceptual framework is required to warrant
 339 meaningful interpretation and comparability of experimental outcomes carried out by research
 340 groups at different institutes. With an emphasis on quality of research, collected data can be
 341 useful far beyond the specific question of a particular experiment. Standardization and
 342 homogenization of terminology, methodology, and data sets could lead to the development of
 343 open-access databases such as those that have been developed for National Institutes of Health
 344 sponsored research in genetics, proteomics, and metabolomics. Enabling meta-analytic studies
 345 is the most economic way of providing robust answers to biological questions (Cooper *et al.*
 346 2009). Vague or ambiguous jargon can lead to confusion and may relegate valuable signals to
 347 wasteful noise. For this reason, measured values must be expressed in standard units for each
 348 parameter used to define mitochondrial respiratory function. Harmonization of nomenclature
 349 and definition of technical terms are essential to improve the awareness of the intricate meaning
 350 of current and past scientific vocabulary, for documentation and integration into databases in
 351 general, and quantitative modelling in particular (Beard 2005). The focus on coupling states
 352 and fluxes through metabolic pathways of aerobic energy transformation in mitochondrial
 353 preparations is a first step in the attempt to generate a conceptually-oriented nomenclature in

or 'will
 support'

354 bioenergetics and mitochondrial physiology. Coupling states of intact cells, the protonmotive
 355 force, and respiratory control by fuel substrates and specific inhibitors of respiratory enzymes
 356 will be reviewed in subsequent communications, prepared In the frame of COST Action
 357 MitoEAGLE open to global bottom-up input.

358
 359

360 2. Coupling states and rates in mitochondrial preparations

361 *‘Every professional group develops its own technical jargon for talking about matters of*
 362 *critical concern ... People who know a word can share that idea with other members of*
 363 *their group, and a shared vocabulary is part of the glue that holds people together and*
 364 *allows them to create a shared culture’ (Miller 1991).*
 365

366 **Mitochondrial preparations** are defined as either isolated mitochondria, or tissue and
 367 cellular preparations in which the barrier function of the plasma membrane is disrupted. Since
 368 this entails the loss of cell viability, mitochondrial preparations are not studied *in vivo*. In
 369 contrast to isolated mitochondria and tissue homogenate preparations, mitochondria in
 370 permeabilized tissues and cells are *in situ* relative to the plasma membrane. The plasma
 371 membrane separates the intracellular compartment including the cytosol, nucleus, and
 372 organelles from the extracellular environment. The plasma membrane consists of a lipid bilayer
 373 with embedded proteins and attached organic molecules that collectively control the selective
 374 permeability of ions, organic molecules, and particles across the cell boundary. The intact
 375 plasma membrane prevents the passage of many water-soluble mitochondrial substrates and
 376 inorganic ions—such as succinate, adenosine diphosphate (ADP) and inorganic phosphate (P_i),
 377 that must be controlled at kinetically-saturating concentrations for the analysis of respiratory
 378 capacities. Despite the activity of solute carriers, e.g., SLC13A3 and SLC20A2, that transport
 379 these metabolites across the plasma membrane of various cell types, this limits the scope of
 380 investigations into mitochondrial respiratory function in intact cells (**Figure 2A**).

381 The cholesterol content of the plasma membrane is high compared to mitochondrial
 382 membranes (Korn 1969). Therefore, mild detergents—such as digitonin and saponin—can be
 383 applied to selectively permeabilize the plasma membrane by interaction with cholesterol and
 384 allow free exchange of organic molecules and inorganic ions between the cytosol and the
 385 immediate cell environment, while maintaining the integrity and localization of organelles,
 386 cytoskeleton, and the nucleus. Application of optimum concentrations of permeabilization
 387 agents (mild detergents or toxins) leads to washout of cytosolic marker enzymes—such as
 388 lactate dehydrogenase—and results in the complete loss of cell viability, tested by nuclear
 389 staining using membrane-impermeable dyes, while mitochondrial function remains intact,
 390 tested by cytochrome *c* addition, for example. Respiration of isolated mitochondria remains
 391 unaltered after the addition of low concentrations of digitonin or saponin, although care should
 392 be taken when isolating mitochondria from cancer cells since they have significantly higher
 393 contents of cholesterol in both membranes (Baggetto and Testa-Perussini, 1990). In addition to
 394 mechanical cell disruption during homogenization of tissue, permeabilization agents may be
 395 applied to ensure permeabilization of all cells in tissue homogenates. Suspensions of cells
 396 permeabilized in the respiration chamber and crude tissue homogenates contain all components
 397 of the cell at highly dilute concentrations. All mitochondria are retained in chemically-
 398 permeabilized mitochondrial preparations and crude tissue homogenates. In the preparation of
 399 isolated mitochondria, however, the mitochondria are separated from other cell fractions and
 400 purified by differential centrifugation, entailing the loss of a fraction of the total mitochondrial
 401 content. Typical mitochondrial recovery ranges from 30% to 80%. Using Percoll or sucrose
 402 density gradients to maximize the purity of isolated mitochondria may compromise the
 403 mitochondrial yield or structural and functional integrity. Therefore, protocols to isolate
 404 mitochondria need to be optimized according to each study. The term mitochondrial preparation

Recent Acta Physiol paper by Lai, Hoppel et al used dispase and trypsin optimize isolation of SS and IM mito's fro muscle

405 does neither include further fractionation of mitochondrial components, nor submitochondrial
406 particles.

if possible move table
closer to this text

408 2.1. Respiratory control and coupling

409
410 Respiratory coupling control states are established in studies of mitochondrial
411 preparations to obtain reference values for various output variables ([Table 1](#)). Physiological
412 conditions *in vivo* deviate from these experimentally obtained states. Since kinetically-
413 saturating concentrations, *e.g.*, of ADP or oxygen (O₂; dioxygen), may not apply to
414 physiological intracellular conditions, relevant information is obtained in studies of kinetic
415 responses to variations in [ADP] or [O₂] in the range between kinetically-saturating
416 concentrations and anoxia (Gnaiger 2001).

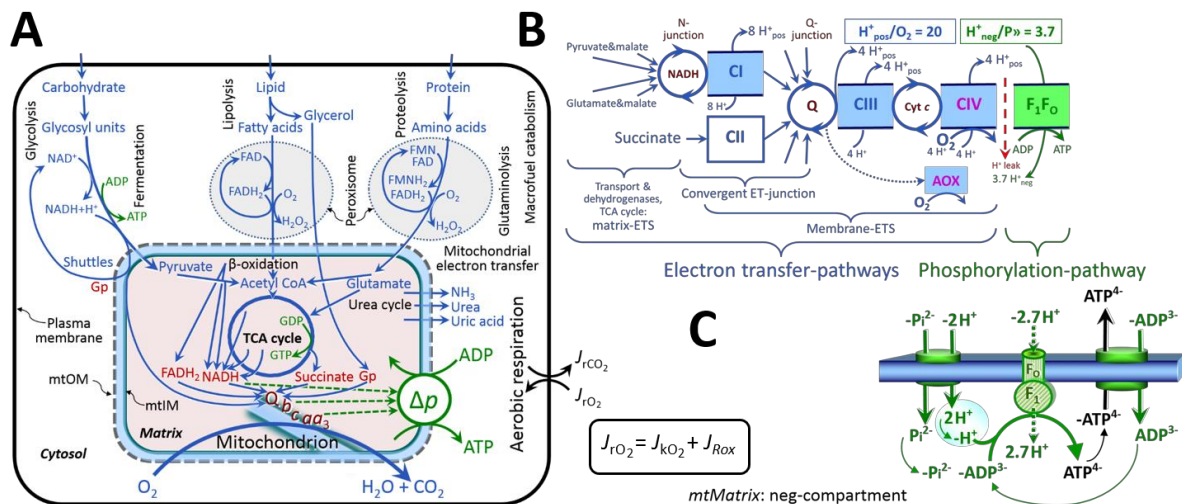
417 **The steady-state:** Mitochondria represent a thermodynamically open system in non-
418 equilibrium states of biochemical energy transformation. State variables (protonmotive force;
419 redox states) and metabolic *rates* (fluxes) are measured in defined mitochondrial respiratory
420 *states*. Steady-states can be obtained only in open systems, in which changes by *internal*
421 transformations, *e.g.*, O₂ consumption, are instantaneously compensated for by *external* fluxes,
422 *e.g.*, O₂ supply, preventing a change of O₂ concentration in the system (Gnaiger 1993b).
423 Mitochondrial respiratory states monitored in closed systems satisfy the criteria of pseudo-
424 steady states for limited periods of time, when changes in the system (concentrations of O₂, fuel
425 substrates, ADP, P_i, H⁺) do not exert significant effects on metabolic fluxes (respiration,
426 phosphorylation). Such pseudo-steady states require respiratory media with sufficient buffering
427 capacity and substrates maintained at kinetically-saturating concentrations, and thus depend on
428 the kinetics of the processes under investigation.

429 **Specification of biochemical dose:** Substrates, uncouplers, inhibitors, and other
430 chemical reagents are titrated to dissect mitochondrial function. Nominal concentrations of
431 these substances are usually reported as initial amount of substance concentration [mol·L⁻¹] in
432 the incubation medium. When aiming at the measurement of kinetically saturated processes—
433 such as OXPHOS-capacities, the concentrations for substrates can be chosen according to the
434 apparent equilibrium constant, K_m' . In the case of hyperbolic kinetics, only 80% of maximum
435 respiratory capacity is obtained at a substrate concentration of four times the K_m' , whereas
436 substrate concentrations of 5, 9, 19 and 49 times the K_m' are theoretically required for reaching
437 83%, 90%, 95% or 98% of the maximal rate (Gnaiger 2001). Other reagents are chosen to
438 inhibit or alter some processes. The amount of these chemicals in an experimental incubation
439 is selected to maximize effect, avoiding unacceptable off-target consequences that would
440 adversely affect the data being sought. Specifying the amount of substance in an incubation as
441 nominal concentration in the aqueous incubation medium can be ambiguous (Doskey *et al.*
442 2015), particularly for lipophilic substances (oligomycin, uncouplers, permeabilization agents)
443 or cations (TPP⁺; fluorescent dyes such as safranin, TMRM; Chowdhury *et al.* 2015), which
444 accumulate in biological membranes or in the mitochondrial matrix. For example, a dose of
445 digitonin of 8 fmol·cell⁻¹ (10 pg·cell⁻¹; 10 μg·10⁻⁶ cells) is optimal for permeabilization of
446 endothelial cells, and the concentration in the incubation medium has to be adjusted according
447 to the cell density applied (Doerrier *et al.* 2018).

448 Generally, dose/exposure can be specified per unit of biological sample, *i.e.*, (nominal
449 moles of xenobiotic)/(number of cells) [mol·cell⁻¹] or, as appropriate, per mass of biological
450 sample [mol·kg⁻¹]. This approach to specification of dose/exposure provides a scalable
451 parameter that can be used to design experiments, help interpret a wide variety of experimental
452 results, and provide absolute information that allows researchers worldwide to make the most
453 use of published data (Doskey *et al.* 2015).

454 **Phosphorylation, P_o, and P_o/O₂ ratio:** *Phosphorylation* in the context of OXPHOS is
455 defined as phosphorylation of ADP by P_i to form ATP. On the other hand, the term

456 phosphorylation is used generally in many contexts, *e.g.*, protein phosphorylation. This justifies
 457 consideration of a symbol more discriminating and specific than P as used in the P/O ratio
 458 (phosphate to atomic oxygen ratio), where P indicates phosphorylation of ADP to ATP or GDP
 459 to GTP (**Figure 2**). We propose the symbol P» for the endergonic (uphill) direction of
 460 phosphorylation ADP→ATP, and likewise the symbol P« for the corresponding exergonic
 461 (downhill) hydrolysis ATP→ADP (**Figure 3**). P» refers mainly to electrontransfer
 462 phosphorylation but may also involve substrate-level phosphorylation as part of the
 463 tricarboxylic acid (TCA) cycle (succinyl-CoA ligase; phosphoglycerate kinase) and
 464 phosphorylation of ADP catalyzed by pyruvate kinase, and of GDP phosphorylated by
 465 phosphoenolpyruvate carboxykinase. Transphosphorylation is performed by adenylate kinase,
 466 creatine kinase (mtCK), hexokinase and nucleoside diphosphate kinase. In isolated mammalian
 467 mitochondria, ATP production catalyzed by adenylate kinase (2 ADP ↔ ATP + AMP) proceeds
 468 without fuel substrates in the presence of ADP (Komlódi and Tretter 2017). Kinase cycles are
 469 involved in intracellular energy transfer and signal transduction for regulation of energy flux.
 470



471 **Figure 2. Cell respiration and oxidative phosphorylation (OXPHOS)**
 472 Mitochondrial respiration is the oxidation of fuel substrates (electron donors) with electron
 473 transfer to O₂ as the electron acceptor. For explanation of symbols see also **Figure 1**.
 474 **(A)** Respiration of intact cells: Extra-mitochondrial catabolism of macrofuels or uptake of small
 475 molecules by the cell provides the *mitochondrial* fuel substrates. Many fuel substrates are
 476 catabolized to acetyl-CoA or to glutamate, and further electron transfer reduces nicotinamide
 477 adenine dinucleotide to NADH or flavin adenine dinucleotide to FADH₂. In respiration,
 478 electron transfer is coupled to the phosphorylation of ADP to ATP, with energy transformation
 479 mediated by the protonmotive force, Δp. Anabolic reactions are linked to catabolism, both by
 480 ATP as the intermediary energy currency and by small organic precursor molecules as building
 481 blocks for biosynthesis (not shown). Glycolysis involves substrate-level phosphorylation of
 482 ADP to ATP in fermentation without utilization of O₂. In contrast, extra-mitochondrial
 483 oxidation of fatty acids and amino acids proceeds partially in peroxisomes without coupling to
 484 ATP production: acyl-CoA oxidase catalyzes the oxidation of FADH₂ with electron transfer to
 485 O₂; amino acid oxidases oxidize flavin mononucleotide FMNH₂ or FADH₂. Coenzyme Q, Q,
 486 and the cytochromes *b*, *c*, and *aa₃* are redox systems of the mitochondrial inner membrane,
 487 mtIM. Dashed arrows indicate the connection between the redox proton pumps (respiratory
 488 Complexes CI, CIII and CIV) and the transmembrane Δp. Mitochondrial outer membrane,
 489 mtOM; glycerol-3-phosphate, Gp; tricarboxylic acid cycle, TCA cycle.
 490 **(B)** Respiration in mitochondrial preparations: The mitochondrial electron transfer system
 491 (ETS) is (1) fuelled by diffusion and transport of substrates across the mitochondrial outer and
 492 inner membrane, and in addition consists of the (2) matrix-ETS, and (3) membrane-ETS.
 493

494 Upstream sections of ET-pathways converge at the N-junction. NADH mainly generated in the
 495 TCA cycle is oxidized by CI and electron entry into the Q-junction. Similarly, succinate is
 496 formed in the TCA cycle and oxidized by CII to fumarate. CII is part of both the TCA cycle
 497 and the ETS, and reduces FAD to FADH₂ with further reduction of ubiquinone to ubiquinol
 498 downstream of the TCA cycle in the Q-junction. Thus FADH₂ is not a substrate but is the
 499 product of CII, in contrast to erroneous metabolic maps shown in many textbooks and
 500 publications. Unspecified arrows converging at the Q-junction indicate additional ET-sections
 501 with electron entry into Q through electron transferring flavoprotein, glycerophosphate
 502 dehydrogenase, dihydro-orotate dehydrogenase, proline dehydrogenase, choline
 503 dehydrogenase, and sulfide-ubiquinone oxidoreductase. The dotted arrow indicates the
 504 branched pathway of oxygen consumption by alternative quinol oxidase (AOX). ET-pathways
 505 are coupled to the phosphorylation-pathway. The H⁺_{pos}/O₂ ratio is the outward proton flux from
 506 the matrix space to the positively (pos) charged vesicular compartment, divided by catabolic
 507 O₂ flux in the NADH-pathway. The H⁺_{neg}/P_» ratio is the inward proton flux from the inter-
 508 membrane space to the negatively (neg) charged matrix space, divided by the flux of
 509 phosphorylation of ADP to ATP. These stoichiometries are not fixed due to ion leaks and proton
 510 slip. Modified from (B) Lemieux *et al.* (2017) and Rich (2013).

511 (C) Chemiosmotic phosphorylation-pathway catalyzed by the proton pump F₁F₀-ATPase (F-
 512 ATPase, ATP synthase), adenine nucleotide translocase, and inorganic phosphate transporter.
 513 The H⁺_{neg}/P_» stoichiometry is the sum of the coupling stoichiometry in the F-ATPase reaction
 514 (-2.7 H⁺_{pos} from the positive intermembrane space, 2.7 H⁺_{neg} to the matrix, *i.e.*, the negative
 515 compartment) and the proton balance in the translocation of ADP³⁻, ATP⁴⁻ and P_i²⁻. Modified
 516 from Gnaiger (2014).

517
 518 The P_»/O₂ ratio (P_»/4 e⁻) is two times the ‘P/O’ ratio (P_»/2 e⁻) of classical bioenergetics.
 519 P_»/O₂ is a generalized symbol, not specific for determination of P_i consumption (P_i/O₂ flux
 520 ratio), ADP depletion (ADP/O₂ flux ratio), or ATP production (ATP/O₂ flux ratio). The
 521 mechanistic P_»/O₂ ratio—or P_»/O₂ stoichiometry—is calculated from the proton-to-O₂ and
 522 proton-to-phosphorylation coupling stoichiometries (**Figure 2B**):
 523

$$524 \quad P_{\gg}/O_2 = \frac{H_{\text{pos}}^+/O_2}{H_{\text{neg}}^+/P_{\gg}} \quad (1)$$

525
 526 The H⁺_{pos}/O₂ *coupling stoichiometry* (referring to the full 4 electron reduction of O₂) depends
 527 on the relative involvement of the three coupling sites (respiratory Complexes I, III and IV; CI,
 528 CIII and CIV) in the catabolic ET-pathway from reduced fuel substrates (electron donors) to
 529 the reduction of O₂ (electron acceptor). This varies with: (1) a bypass of CI by single or multiple
 530 electron input into the Q-junction; and (2) a bypass of CIV by involvement of alternative
 531 oxidases, AOX, which are not expressed in mammalian mitochondria.

532 H⁺_{pos}/O₂ is 12 in the ET-pathways involving CIII and CIV as proton pumps, increasing to
 533 20 for the NADH-pathway through CI (**Figure 2B**), but a general consensus on H⁺_{pos}/O₂
 534 stoichiometries remains to be reached (Hinkle 2005; Wikström and Hummer 2012; Sazanov
 535 2015). The H⁺_{neg}/P_» coupling stoichiometry (3.7; **Figure 2B**) is the sum of 2.7 H⁺_{neg} required
 536 by the F-ATPase of vertebrate and most invertebrate species (Watt *et al.* 2010) and the proton
 537 balance in the translocation of ADP, ATP and P_i (**Figure 2C**). Taken together, the mechanistic
 538 P_»/O₂ ratio is calculated at 5.4 and 3.3 for NADH- and succinate-linked respiration,
 539 respectively (Eq. 1). The corresponding classical P_»/O ratios (referring to the 2 electron
 540 reduction of 0.5 O₂) are 2.7 and 1.6 (Watt *et al.* 2010), in agreement with the measured P_»/O
 541 ratio for succinate of 1.58 ± 0.02 (Gnaiger *et al.* 2000).

542 The effective P_»/O₂ flux ratio ($\dot{Y}_{P_{\gg}/O_2} = J_{P_{\gg}}/J_{kO_2}$; **Figure 3**) is diminished relative to the
 543 mechanistic P_»/O₂ ratio by intrinsic and extrinsic uncoupling *versus* dyscoupling (**Figure 4**).
 544 Such generalized uncoupling is different from switching to mitochondrial pathways that involve

545 fewer than three proton pumps ('coupling sites': Complexes CI, CIII and CIV), bypassing CI
 546 through multiple electron entries into the Q-junction, or CIII and CIV through AOX (**Figure**
 547 **2B**). Reprogramming of mitochondrial pathways leading to different types of substrates being
 548 oxidized may be considered as a switch of gears (changing the stoichiometry by altering the
 549 substrate that is oxidized) rather than uncoupling (loosening the tightness of coupling relative
 550 to a fixed stoichiometry). In addition, $Y_{P\gg O_2}$ depends on several experimental conditions of flux
 551 control, increasing as a hyperbolic function of [ADP] to a maximum value (Gnaiger 2001).

552 **Control and regulation:** The terms metabolic *control* and *regulation* are frequently used
 553 synonymously, but are distinguished in metabolic control analysis: 'We could understand the
 554 regulation as the mechanism that occurs when a system maintains some variable constant over
 555 time, in spite of fluctuations in external conditions (homeostasis of the internal state). On the
 556 other hand, metabolic control is the power to change the state of the metabolism in response to
 557 an external signal' (Fell 1997). Respiratory control may be induced by experimental control
 558 signals that *exert* an influence on: (1) ATP demand and ADP phosphorylation-rate; (2) fuel
 559 substrate composition, pathway competition; (3) available amounts of substrates and O₂, *e.g.*,
 560 starvation and hypoxia; (4) the protonmotive force, redox states, flux–force relationships,
 561 coupling and efficiency; (5) Ca²⁺ and other ions including H⁺; (6) inhibitors, *e.g.*, nitric oxide
 562 or intermediary metabolites such as oxaloacetate; (7) signalling pathways and regulatory
 563 proteins, *e.g.*, insulin resistance, transcription factor hypoxia inducible factor 1. *Mechanisms* of
 564 respiratory control and regulation include adjustments of: (1) enzyme activities by allosteric
 565 mechanisms and phosphorylation; (2) enzyme content, concentrations of cofactors and
 566 conserved moieties—such as adenylates, nicotinamide adenine dinucleotide [NAD⁺/NADH],
 567 coenzyme Q, cytochrome *c*; (3) metabolic channeling by supercomplexes; and (4)
 568 mitochondrial density (enzyme concentrations and membrane area) and morphology (cristae
 569 folding, fission and fusion). Mitochondria are targeted directly by hormones, *e.g.*, progesterone
 570 and glucacorticoids, which affect their energy metabolism (Lee *et al.* 2013; Gerö and Szabo
 571 2016; Price and Dai 2016; Moreno *et al.* 2017). Evolutionary or acquired differences in the
 572 genetic and epigenetic basis of mitochondrial function (or dysfunction) between individuals;
 573 age; gender, biological sex, and hormone concentrations; life style including exercise and
 574 nutrition; and environmental issues including thermal, atmospheric, toxic and pharmacological
 575 factors, exert an influence on all control mechanisms listed above. For reviews, see Brown
 576 1992; Gnaiger 1993a, 2009; 2014; Paradies *et al.* 2014; Morrow *et al.* 2017.

577 **Respiratory control and response:** Lack of control by a metabolic pathway, *e.g.*,
 578 phosphorylation-pathway, means that there will be no response to a variable activating it, *e.g.*,
 579 [ADP]. The reverse, however, is not true as the absence of a response to [ADP] does not exclude
 580 the phosphorylation-pathway from having some degree of control. The degree of control of a
 581 component of the OXPHOS-pathway on an output variable—such as O₂ flux, will in general
 582 be different from the degree of control on other outputs—such as phosphorylation-flux or
 583 proton leak flux. Therefore, it is necessary to be specific as to which input and output are under
 584 consideration (Fell 1997). — perhaps offer and example here?

585 **Respiratory coupling control and ET-pathway control:** Respiratory control refers to
 586 the ability of mitochondria to adjust O₂ flux in response to external control signals by engaging
 587 various mechanisms of control and regulation. Respiratory control is monitored in a
 588 mitochondrial preparation under conditions defined as respiratory states, preferentially under
 589 near-physiological conditions of O₂ concentration, pH, temperature and medium ionic
 590 composition, to generate data of higher biological relevance. When phosphorylation of ADP to
 591 ATP is stimulated or depressed, an increase or decrease is observed in electron transfer
 592 measured as O₂ flux in respiratory coupling states of intact mitochondria ('controlled states' in
 593 the classical terminology of bioenergetics). Alternatively, coupling of electron transfer with
 594 phosphorylation is disengaged by uncouplers. These protonophores are weak lipid-soluble acids
 595 which disrupt the barrier function of the mtIM and thus short circuit the protonmotive system.

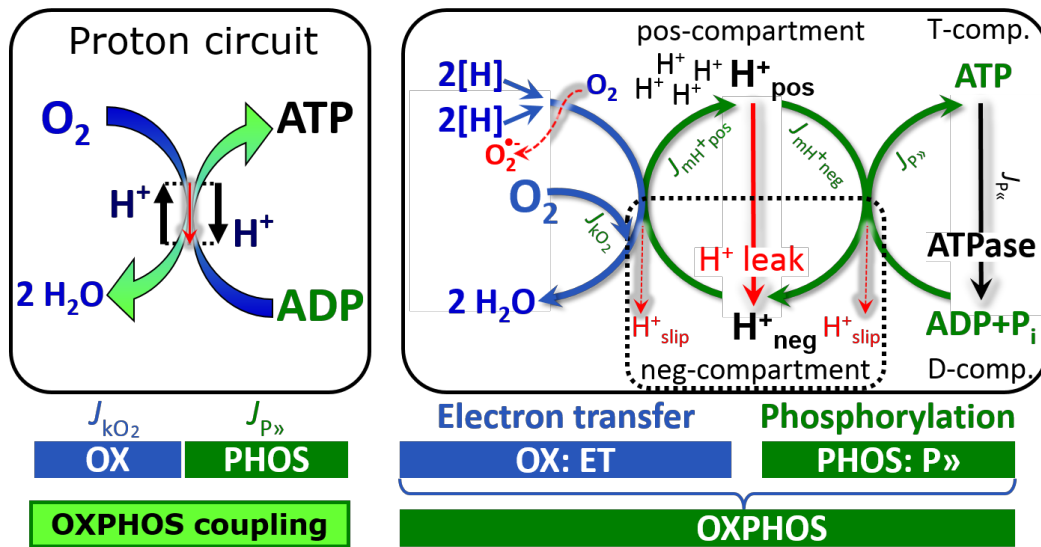
'diminished'

To me gender is a sociological term that reflects ones choice to identify as male, female, gender fluid etc. No sure the relevance of gender here, particularly next to biological sex.

13

Should UCPs be mentioned here since they play a very specific physiological role in coupling control?

596 functioning like a clutch in a mechanical system. The corresponding coupling control state is
 597 characterized by a high O₂ flux without control by P» (noncoupled or ‘uncontrolled state’).
 598
 599



600 **Figure 3. Coupling in oxidative phosphorylation (OXPHOS)**
 601 2[H] indicates the reduced hydrogen equivalents of fuel substrates of the catabolic reaction k
 602 with oxygen. O₂ flux, J_{kO_2} , through the catabolic ET-pathway, is coupled to flux through the
 603 phosphorylation-pathway of ADP to ATP, $J_{P»}$. The redox proton pumps of the ET-pathway
 604 drive proton flux into the positive (pos) compartment, J_{mH^+pos} , generating the output
 605 protonmotive force (motive, subscript m). F-ATPase is coupled to inward proton current into
 606 the negative (neg) compartment, J_{mH^+neg} , to phosphorylate ADP to ATP. The system is defined
 607 by the boundaries (full black line) and is not a black box, but is analysed as a compartmental
 608 system. The negative compartment (neg-compartment, enclosed by the dotted line) is the
 609 matrix space, separated by the mtIM from the positive compartment (pos-compartment).
 610 ADP+P_i and ATP are the substrate- and product-compartments (scalar ADP and ATP
 611 compartments, D-comp. and T-comp.), respectively. At steady-state proton turnover, $J_{\infty H^+}$, and
 612 ATP turnover, $J_{\infty P}$, maintain concentrations constant, when $J_{mH^+\infty} = J_{mH^+pos} = J_{mH^+neg}$, and $J_{P\infty}$
 613 = $J_{P»} = J_{P«}$. Modified from Gnaiger (2014).

614
 615 ET-pathway control states are obtained in mitochondrial preparations by depletion of
 616 endogenous substrates and addition to the mitochondrial respiration medium of fuel substrates
 617 (Figure 2; 2[H] in Figure 3) and specific inhibitors, activating selected mitochondrial catabolic
 618 pathways, k, of electron transfer from the oxidation of fuel substrates to reduction of O₂ (Figure
 619 2A). Coupling control states and pathway control states are complementary, since
 620 mitochondrial preparations depend on an exogenous supply of pathway-specific fuel substrates
 621 and oxygen (Gnaiger 2014).

622 **Coupling:** In mitochondrial electron transfer, vectorial transmembrane proton flux is
 623 coupled through the redox proton pumps CI, CIII and CIV to the catabolic flux of scalar
 624 reactions, collectively measured as O₂ flux (Figure 3). Thus mitochondria are elementary
 625 components of energy transformation. Energy is a conserved quantity and cannot be lost or
 626 produced in any internal process (First Law of thermodynamics). Open and closed systems can
 627 gain or lose energy only by external fluxes—by exchange with the environment. Therefore,
 628 energy can neither be produced by mitochondria, nor is there any internal process without
 629 energy conservation. Exergy or Gibbs energy (‘free energy’) is the part of energy that can
 630 potentially be transformed into work under conditions of constant volume and pressure.
 631 *Coupling* is the interaction of an exergonic process (spontaneous, negative exergy change) with

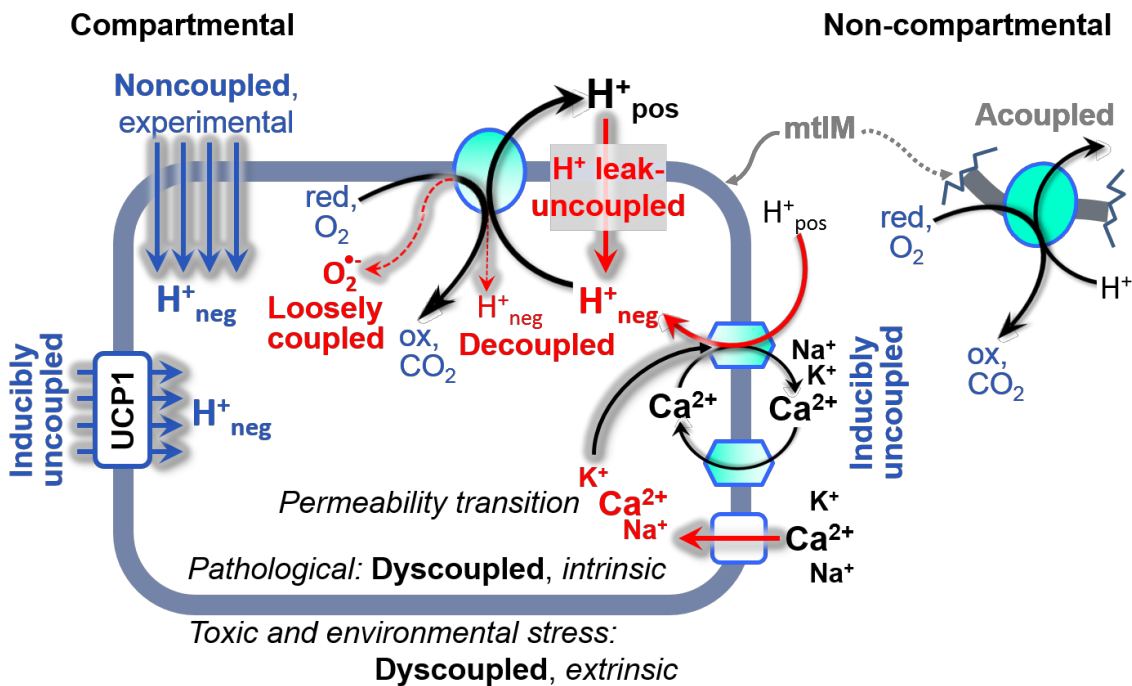
632 an endergonic process (positive exergy change) in energy transformations which conserve part
 633 of the exergy that would be irreversibly lost or dissipated in an uncoupled process.

634 **Uncoupling:** Uncoupling of mitochondrial respiration is a general term comprising
 635 diverse mechanisms:

- 636 1. Proton leak across the mtIM from the pos- to the neg-compartment (H^+ leak-
 637 uncoupled; **Figure 4**).
- 638 2. Cycling of other cations, strongly stimulated by permeability transition; comparable
 639 to the use of protonophores, cation cycling is experimentally induced by valinomycin
 640 in the presence of K^+ ;
- 641 3. Decoupling by proton slip in the redox proton pumps when protons are effectively not
 642 pumped (CI, CIII and CIV) or are not driving phosphorylation (F-ATPase);
- 643 4. Loss of vesicular (compartmental) integrity when electron transfer is uncoupled;
- 644 5. Electron leak in the loosely coupled univalent reduction of O_2 to superoxide ($O_2^{\bullet-}$;
 645 superoxide anion radical).

646 Differences of terms—uncoupled vs. noncoupled—are easily overlooked, although they relate
 647 to different meanings of uncoupling (**Figure 4** and **Table 2**).

648
 649



650
 651
 652
 653
 654
 655
 656
 657
 658
 659
 660
 661
 662
 663
 664

Figure 4. Mechanisms of respiratory uncoupling

An intact mitochondrial inner membrane, mtIM, is required for vectorial, compartmental coupling. ‘Acoupled’ respiration is the consequence of structural disruption with catalytic activity of non-compartmental mitochondrial fragments. Inducibly uncoupled (activation of UCP1) and experimentally noncoupled respiration (titration of protonophores) stimulate respiration to maximum O_2 flux. H^+ leak-uncoupled, decoupled, and loosely coupled respiration are components of intrinsic uncoupling (**Table 2**). Pathological dysfunction may affect all types of uncoupling, including permeability transition, causing intrinsically dyscoupled respiration. Similarly, toxicological and environmental stress factors can cause extrinsically dyscoupled respiration. Reduced fuel substrates, red; oxidized products, ox.

665 2.2. Coupling states and respiratory rates

666

667

668 **Respiratory capacities in coupling control states:** To extend the classical nomenclature
 669 on mitochondrial coupling states (Section 2.3) by a concept-driven terminology that explicitly
 670 incorporates information on the meaning of respiratory states, the terminology must be general
 671 and not restricted to any particular experimental protocol or mitochondrial preparation (Gnaiger
 672 2009). Concept-driven nomenclature aims at mapping the *meaning and concept behind the*
 673 *words and acronyms onto the forms of words and acronyms* (Miller 1991). The focus of
 674 concept-driven nomenclature is primarily the conceptual ‘why’, along with clarification of the
 675 experimental ‘how’. Respiratory capacities delineate, comparable to channel capacity in
 676 information theory (Schneider 2006), the upper bound of the rate of respiration measured in
 677 defined coupling control states and electron transfer-pathway (ET-pathway) states (**Figure 5**).

677

678

679

680 **Figure 5. Four-compartment** 681 **model of oxidative** 682 **phosphorylation**

682 Respiratory states (ET,

683 OXPPOS, LEAK; **Table 1**) and684 corresponding rates (E , P , L) are

685 connected by the protonmotive

686 force, Δp . (1) ET-capacity, E , is

687 partitioned into (2) dissipative

688 LEAK-respiration, L , when the

689 Gibbs energy change of catabolic

690 O_2 flux is irreversibly lost, (3) net691 OXPPOS-capacity, $P-L$, with partial

692 conservation of the capacity to

693 perform work, and (4) the excess

694 capacity, $E-P$. Modified from Gnaiger (2014).

695

696

697

698

699

700

701

702

703

704

705

706

707

708

709

710

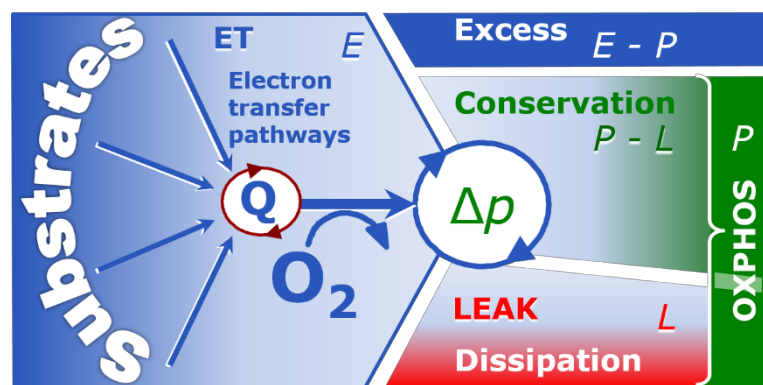
711

712

713

714

715



694 To provide a diagnostic reference for respiratory capacities of core energy metabolism,
 695 the capacity of *oxidative phosphorylation*, OXPPOS, is measured at kinetically-saturating
 696 concentrations of ADP and P_i . The *oxidative* ET-capacity reveals the limitation of OXPPOS-
 697 capacity mediated by the *phosphorylation*-pathway. The ET- and phosphorylation-pathways
 698 comprise coupled segments of the OXPPOS-system. ET-capacity is measured as noncoupled
 699 respiration by application of *external uncouplers*. The contribution of *intrinsically uncoupled*
 700 O_2 consumption is studied by preventing the stimulation of phosphorylation either in the
 701 absence of ADP or by inhibition of the phosphorylation-pathway. The corresponding states are
 702 collectively classified as LEAK-states, when O_2 consumption compensates mainly for ion
 703 leaks, including the proton leak. Defined coupling states are induced by: (1) adding cation
 704 chelators such as EGTA, binding free Ca^{2+} and thus limiting cation cycling; (2) adding ADP
 705 and P_i ; (3) inhibiting the phosphorylation-pathway; and (4) uncoupler titrations, while
 706 maintaining a defined ET-pathway state with constant fuel substrates and inhibitors of specific
 707 branches of the ET-pathway (**Figure 5**).

708 The three coupling states, ET, LEAK and OXPPOS, are shown schematically with the
 709 corresponding respiratory rates, abbreviated as E , L and P , respectively (**Figure 5**). We
 710 distinguish metabolic *pathways* from metabolic *states* and the corresponding metabolic *rates*;
 711 for example: ET-pathways, ET-states, and ET-capacities, E , respectively (**Table 1**). The
 712 protonmotive force is *high* in the OXPPOS-state when it drives phosphorylation, *maximum* in
 713 the LEAK-state of coupled mitochondria, driven by LEAK-respiration at a minimum back-flux
 714 of cations to the matrix side, and *very low* in the ET-state when uncouplers short-circuit the
 715 proton cycle (**Table 1**).

716 **LEAK-state (Figure 6A):**
 717 The LEAK-state is defined as a
 718 state of mitochondrial respiration
 719 when O_2 flux mainly
 720 compensates for ion leaks in the
 721 absence of ATP synthesis, at
 722 kinetically-saturating
 723 concentrations of O_2 , respiratory
 724 fuel substrates and P_i . LEAK-
 725 respiration is measured to obtain
 726 an estimate of *intrinsic*
 727 *uncoupling* without addition of an
 728 experimental uncoupler: (1) in the
 729 absence of adenylates, *i.e.*, AMP,
 730 ADP and ATP; (2) after depletion
 731 of ADP at a maximum ATP/ADP
 732 ratio; or (3) after inhibition of the
 733 phosphorylation-pathway by
 734 inhibitors of F-ATPase—such as
 735 oligomycin, or of adenine
 736 nucleotide translocase—such as
 737 carboxyatractyloside.
 738 Adjustment of the nominal
 739 concentration of these inhibitors
 740 to the density of biological
 741 sample applied can minimize or
 742 avoid inhibitory side-effects
 743 exerted on ET-capacity or even
 744 some dyscoupling.

745 • **Proton leak and uncoupled respiration:**

746 The intrinsic proton leak is
 747 the *uncoupled* leak current
 748 of protons in which
 749 protons diffuse across the
 750 mtIM in the dissipative
 751 direction of the downhill
 752 protonmotive force
 753 without coupling to
 754 phosphorylation (Figure
 755 6A). The proton leak flux
 756 depends non-linearly on
 757 the protonmotive force
 758 (Garlid *et al.* 1989;
 759 Divakaruni and Brand
 760 2011), it is a temperature-
 761 dependent property of the
 762 mtIM and may be enhanced
 763 due to possible contaminations
 764 by free fatty acids. Inducible
 765 uncoupling mediated by
 766 uncoupling protein 1 (UCP1) is
 physiologically controlled, *e.g.*,
 in brown adipose tissue. UCP1
 is a member of the mitochondrial
 carrier family that is involved
 in the translocation of protons
 across the mtIM (Klingenberg
 2017).

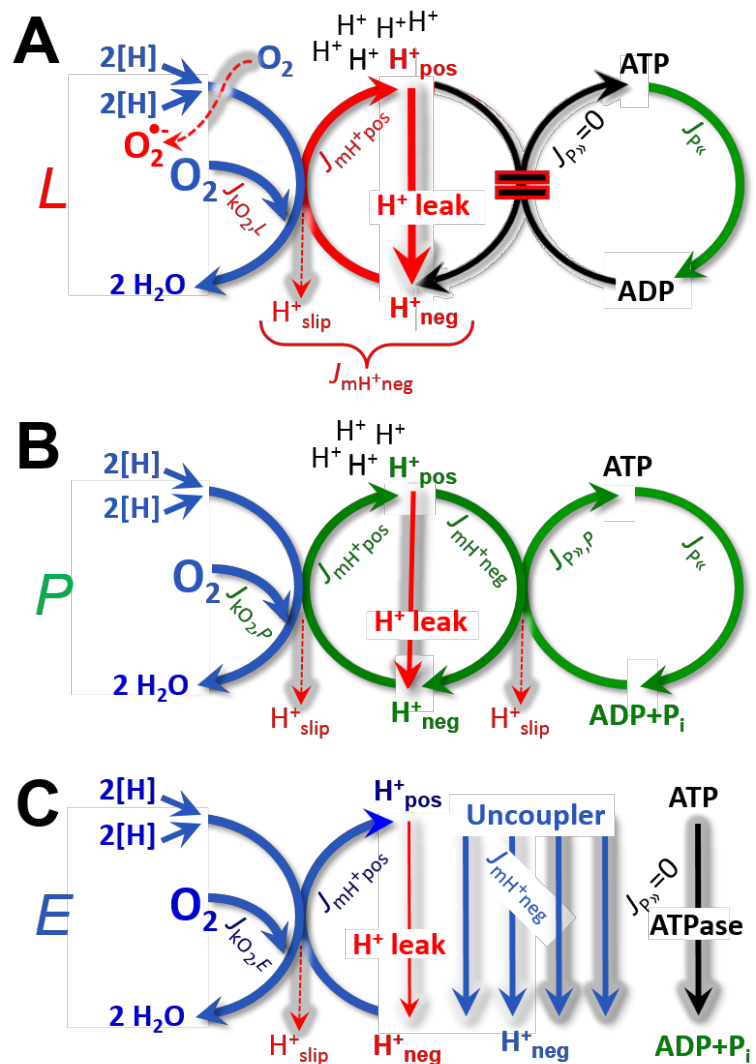


Figure 6. Respiratory coupling states

(A) **LEAK-state and rate, *L***: Phosphorylation is arrested, $J_{P\gg} = 0$, and catabolic O_2 flux, $J_{kO_2,L}$, is controlled mainly by the proton leak, $J_{mH^+neg,L}$, at maximum protonmotive force (Figure 4). Extramitochondrial ATP may be hydrolyzed by extramitochondrial ATPases, $J_{P\ll}$.

(B) **OXPHOS-state and rate, *P***: Phosphorylation, $J_{P\gg}$, is stimulated by kinetically-saturating [ADP] and [P_i], and is supported by a high protonmotive force. O_2 flux, $J_{kO_2,P}$, is well-coupled at a $P\gg/O_2$ ratio of $J_{P\gg,P}/J_{kO_2,P}$. Extramitochondrial ATPases may recycle ATP, $J_{P\ll}$.

(C) **ET-state and rate, *E***: Noncoupled respiration, $J_{kO_2,E}$, is maximum at optimum exogenous uncoupler concentration and phosphorylation is zero, $J_{P\gg} = 0$. The F-ATPase may hydrolyze extramitochondrial ATP. See also Figure 3.

'this short-circuit drives electron transfer and respiration in the absence of ADP phosphorylation, dissipating membrane potential as heat.

767 Consequently, the short-circuit diminishes the protonmotive force and stimulates electron
 768 transfer to O₂ and heat dissipation without phosphorylation of ADP.

- 769 • **Cation cycling:** There can be other cation contributors to leak current including calcium
 770 and probably magnesium. Calcium influx is balanced by mitochondrial Na⁺/Ca²⁺ or
 771 H⁺/Ca²⁺ exchange, which is balanced by Na⁺/H⁺ or K⁺/H⁺ exchanges. This is another
 772 effective uncoupling mechanism different from proton leak (**Table 2**).
 773

774 **Table 1. Coupling states and residual oxygen consumption in mitochondrial**
 775 **preparations in relation to respiration- and phosphorylation-flux, J_{kO_2} and $J_{P_{\gg}}$,**
 776 **and protonmotive force, Δp .** Coupling states are established at kinetically-
 777 saturating concentrations of fuel substrates and O₂.

State	J_{kO_2}	$J_{P_{\gg}}$	Δp	Inducing factors	Limiting factors
LEAK	L ; low, cation leak-dependent respiration	0	max.	back-flux of cations including proton leak, proton slip	$J_{P_{\gg}} = 0$: (1) without ADP, L_N ; (2) max. ATP/ADP ratio, L_T ; or (3) inhibition of the phosphorylation-pathway, L_{Omy}
OXPHOS	P ; high, ADP-stimulated respiration	max.	high	kinetically-saturating [ADP] and [P _i]	$J_{P_{\gg}}$ by phosphorylation-pathway; or J_{kO_2} by ET-capacity
ET	E ; max., noncoupled respiration	0	low	optimal external uncoupler concentration for max. $J_{O_2,E}$	J_{kO_2} by ET-capacity
ROX	R_{ox} ; min., residual O ₂ consumption	0	0	$J_{O_2,Rox}$ in non-ET-pathway oxidation reactions	inhibition of all ET-pathways; or absence of fuel substrates

- 778
- 779 • **Proton slip and decoupled respiration:** Proton slip is the *decoupled* process in which
 780 protons are only partially translocated by a redox proton pump of the ET-pathways and
 781 slip back to the original vesicular compartment. The proton leak is the dominant
 782 contributor to the overall leak current in mammalian mitochondria incubated under
 783 physiological conditions at 37 °C, whereas proton slip is increased at lower experimental
 784 temperature (Canton *et al.* 1995). Proton slip can also happen in association with the F-
 785 ATPase, in which the proton slips downhill across the pump to the matrix without
 786 contributing to ATP synthesis. In each case, proton slip is a property of the proton pump
 787 and increases with the pump turnover rate.
- 788 • **Electron leak and loosely coupled respiration:** Superoxide production by the ETS leads
 789 to a bypass of redox proton pumps and correspondingly lower P_»/O₂ ratio. This depends
 790 on the actual site of electron leak and the scavenging of hydrogen peroxide by cytochrome
 791 *c*, whereby electrons may re-enter the ETS with proton translocation by CIV.
- 792 • **Loss of compartmental integrity and acoupled respiration:** Electron transfer and
 793 catabolic O₂ flux proceed without compartmental proton translocation in disrupted
 794 mitochondrial fragments. Such fragments form during mitochondrial isolation, and may
 795 not fully fuse to re-establish structurally intact mitochondria. Loss of mtIM integrity,
 796 therefore, is the cause of acoupled respiration, which is a nonvectorial dissipative process
 797 without control by the protonmotive force.

- 798 • **Dyscoupled respiration:** Mitochondrial injuries may lead to *dyscoupling* as a
 799 pathological or toxicological cause of *uncoupled* respiration. Dyscoupling may involve
 800 any type of uncoupling mechanism, *e.g.*, opening the permeability transition pore.
 801 Dyscoupled respiration is distinguished from the experimentally induced *noncoupled*
 802 respiration in the ET-state (**Table 2**).
 803
 804

Table 2. Terms on respiratory coupling and uncoupling.

Term	J_{kO_2}	$P \gg O_2$	Notes	
acoupled		0	electron transfer in mitochondrial fragments without vectorial proton translocation (Figure 4)	
intrinsic, no protonophore added	uncoupled	L	0	non-phosphorylating LEAK-respiration (Figure 6A)
	proton leak-uncoupled		0	component of L , H^+ diffusion across the mtIM (Figure 4)
	decoupled		0	component of L , proton slip (Figure 4)
	loosely coupled		0	component of L , lower coupling due to superoxide formation and bypass of proton pumps by electron leak (Figure 4)
	dyscoupled		0	pathologically, toxicologically, environmentally increased uncoupling, mitochondrial dysfunction
	inducibly uncoupled		0	by UCP1 or cation (<i>e.g.</i> , Ca^{2+}) cycling (Figure 4) does ANT need to also be mentioned here?
noncoupled	E	0	non-phosphorylating respiration stimulated to maximum flux at optimum exogenous uncoupler concentration (Figure 6C)	
well-coupled	P	high	phosphorylating respiration with an intrinsic LEAK component (Figure 6B)	
fully coupled	$P - L$	max.	OXPHOS-capacity corrected for LEAK-respiration (Figure 5)	

805

806

807

808

809

810

811

812

813

814

815

816

817

818

819

820

821

OXPHOS-state (Figure 6B): The OXPHOS-state is defined as the respiratory state with kinetically-saturating concentrations of O_2 , respiratory and phosphorylation substrates, and absence of exogenous uncoupler, which provides an estimate of the maximal respiratory capacity in the OXPHOS-state for any given ET-pathway state. Respiratory capacities at kinetically-saturating substrate concentrations provide reference values or upper limits of performance, aiming at the generation of data sets for comparative purposes. Physiological activities and effects of substrate kinetics can be evaluated relative to the OXPHOS-capacity.

As discussed previously, 0.2 mM ADP does not fully saturate flux in isolated mitochondria (Gnaiger 2001; Puchowicz *et al.* 2004); greater ADP concentration is required, particularly in permeabilized muscle fibres and cardiomyocytes, to overcome limitations by intracellular diffusion and by the reduced conductance of the mtOM (Jepihhina *et al.* 2011, Illaste *et al.* 2012, Simson *et al.* 2016), either through interaction with tubulin (Rostovtseva *et al.* 2008) or other intracellular structures (Birkedal *et al.* 2014). In addition, saturating ADP concentrations need to be evaluated under different experimental conditions such as temperature (Lemieux *et al.* 2017) and with different animal models (Blier and Guderley,

822 1993). In permeabilized muscle fibre bundles of high respiratory capacity, the apparent K_m for
 823 ADP increases up to 0.5 mM (Saks *et al.* 1998), consistent with experimental evidence that
 824 >90% saturation is reached only at >5 mM ADP (Pesta and Gnaiger 2012). Similar ADP
 825 concentrations are also required for accurate determination of OXPHOS-capacity in human
 826 clinical cancer samples and permeabilized cells (Klepinin *et al.* 2016; Koit *et al.* 2017).
 827 Whereas 2.5 to 5 mM ADP is sufficient to obtain the actual OXPHOS-capacity in many types
 828 of permeabilized tissue and cell preparations, experimental validation is required in each
 829 specific case.

830 **Electron transfer-state (Figure 6C):** O_2 flux determined in the ET-state yields an
 831 estimate of ET-capacity. The ET-state is defined as the *noncoupled* state with kinetically-
 832 saturating concentrations of O_2 , respiratory substrate and optimum *exogenous* uncoupler
 833 concentration for maximum O_2 flux. As a consequence of the nearly collapsed protonmotive
 834 force, the driving force is insufficient for phosphorylation, and $J_{P\gg} = 0$. The most frequently
 835 used uncouplers are carbonyl cyanide *m*-chloro phenyl hydrazone (CCCP), carbonyl cyanide
 836 *p*-trifluoromethoxyphenylhydrazone (FCCP), or dinitrophenole (DNP). Stepwise titration of
 837 uncouplers stimulates respiration up to or above the level of O_2 consumption rates in the
 838 OXPHOS-state, but inhibition of respiration is observed above optimum uncoupler
 839 concentrations (Mitchell 2011). Data obtained with a single dose of uncoupler must be
 840 evaluated with caution, particularly when a fixed uncoupler concentration is used in studies
 841 exploring a treatment or disease that may alter the mitochondrial content or mitochondrial
 842 sensitivity to inhibition by uncouplers. The effect on ET-capacity of the reversed function of F-
 843 ATPase ($J_{P\ll}$; Figure 6C) can be evaluated in the presence and absence of extramitochondrial
 844 ATP.

845 **ROX state and Rox:** Besides the three fundamental coupling states of mitochondrial
 846 preparations, the state of residual O_2 consumption, ROX, is relevant to assess respiratory
 847 function (Figure 1). ROX is not a coupling state. The rate of residual oxygen consumption,
 848 *Rox*, is defined as O_2 consumption due to oxidative reactions measured after inhibition of ET—
 849 with rotenone, malonic acid and antimycin A. Cyanide and azide inhibit not only CIV but
 850 catalase and several peroxidases involved in *Rox*. However, high concentrations of antimycin
 851 A, but not rotenone or cyanide, inhibit peroxisomal acyl-CoA oxidase and D-amino acid
 852 oxidase (Vamecq *et al.* 1987). ROX represents a baseline that is used to correct respiration
 853 measured in defined coupling states. *Rox*-corrected L , P and E not only lower the values of total
 854 fluxes, but also changes the flux control ratios L/P and L/E . *Rox* is not necessarily equivalent
 855 to non-mitochondrial reduction of O_2 , considering O_2 -consuming reactions in mitochondria that
 856 are not related to ET—such as O_2 consumption in reactions catalyzed by monoamine oxidases
 857 (type A and B), monooxygenases (cytochrome P450 monooxygenases), dioxygenase (sulfur
 858 dioxygenase and trimethyllysine dioxygenase), and several hydroxylases. Even isolated
 859 mitochondrial fractions, especially those obtained from liver, may be contaminated by
 860 peroxisomes. This fact makes the exact determination of mitochondrial O_2 consumption and
 861 mitochondria-associated generation of reactive oxygen species complicated (Schönfeld *et al.*
 862 2009; Speijer 2016; Figure 2). The dependence of ROX-linked O_2 consumption needs to be
 863 studied in detail together with non-ET enzyme activities, availability of specific substrates, O_2
 864 concentration, and electron leakage leading to the formation of reactive oxygen species.

865 **Quantitative relations:** E may exceed or be equal to P . $E > P$ is observed in many types
 866 of mitochondria, varying between species, tissues and cell types (Gnaiger 2009). $E - P$ is the
 867 excess ET-capacity pushing the phosphorylation-flux (Figure 2C) to the limit of its *capacity of*
 868 *utilizing* the protonmotive force. In addition, the magnitude of $E - P$ depends on the tightness of
 869 respiratory coupling or degree of uncoupling, since an increase of L causes P to increase
 870 towards the limit of E . The *excess* $E - P$ capacity, $E - P$, therefore, provides a sensitive diagnostic
 871 indicator of specific injuries of the phosphorylation-pathway, under conditions when E remains
 872 constant but P declines relative to controls (Figure 5). Substrate cocktails supporting

873 simultaneous convergent electron transfer to the Q-junction for reconstitution of TCA cycle
 874 function establish pathway control states with high ET-capacity, and consequently increase the
 875 sensitivity of the *E-P* assay.

876 *E* cannot theoretically be lower than *P*. $E < P$ must be discounted as an artefact, which
 877 may be caused experimentally by: (1) loss of oxidative capacity during the time course of the
 878 respirometric assay, since *E* is measured subsequently to *P*; (2) using insufficient uncoupler
 879 concentrations; (3) using high uncoupler concentrations which inhibit ET (Gnaiger 2008); (4)
 880 high oligomycin concentrations applied for measurement of *L* before titrations of uncoupler,
 881 when oligomycin exerts an inhibitory effect on *E*. On the other hand, the excess ET-capacity is
 882 overestimated if non-saturating [ADP] or [P_i] are used. See State 3 in the next section.

883 The net OXPHOS-capacity is calculated by subtracting *L* from *P* (**Figure 5**). The net
 884 $P \gg O_2$ equals $P \gg (P-L)$, wherein the dissipative LEAK component in the OXPHOS-state may
 885 be overestimated. This can be avoided by measuring LEAK-respiration in a state when the
 886 protonmotive force is adjusted to its slightly lower value in the OXPHOS-state—by titration of
 887 an ET inhibitor (Divakaruni and Brand 2011). Any turnover-dependent components of proton
 888 leak and slip, however, are underestimated under these conditions (Garlid *et al.* 1993). In
 889 general, it is inappropriate to use the term *ATP production* or *ATP turnover* for the difference
 890 of O₂ flux measured in the OXPHOS and LEAK states. *P-L* is the upper limit of OXPHOS-
 891 capacity that is freely available for ATP production (corrected for LEAK-respiration) and is
 892 fully coupled to phosphorylation with a maximum mechanistic stoichiometry (**Figure 5**).

893 The rates of LEAK respiration and OXPHOS capacity depend on (1) the tightness of
 894 coupling under the influence of the respiratory uncoupling mechanisms (**Figure 4**), and (2) the
 895 coupling stoichiometry, which varies as a function of the substrate type undergoing oxidation
 896 in ET-pathways with either two or three coupling sites (**Figure 2B**). When cocktails with
 897 NADH-linked substrates and succinate are used, the relative contribution of ET-pathways with
 898 three or two coupling sites cannot be controlled experimentally, is difficult to determine, and
 899 may shift in transitions between LEAK-, OXPHOS- and ET-states (Gnaiger 2014). Under these
 900 experimental conditions, we cannot separate the tightness of coupling *versus* coupling
 901 stoichiometry as the mechanisms of respiratory control in the shift of *L/P* ratios. The tightness
 902 of coupling and fully coupled O₂ flux, *P-L* (**Table 2**), therefore, are obtained from
 903 measurements of coupling control of LEAK respiration, OXPHOS- and ET-capacities in well
 904 defined pathway states, using either pyruvate and malate as substrates or the classical succinate
 905 and rotenone substrate-inhibitor combination (**Figure 2B**).

906

907 2.3. Classical terminology for isolated mitochondria

908 *‘When a code is familiar enough, it ceases appearing like a code; one forgets that there*
 909 *is a decoding mechanism. The message is identical with its meaning’* (Hofstadter 1979).

910

911 Chance and Williams (1955; 1956) introduced five classical states of mitochondrial
 912 respiration and cytochrome redox states. **Table 3** shows a protocol with isolated mitochondria
 913 in a closed respirometric chamber, defining a sequence of respiratory states. States and rates
 914 are not specifically distinguished in this nomenclature.

915 **State 1** is obtained after addition of isolated mitochondria to air-saturated
 916 isoosmotic/isotonic respiration medium containing P_i, but no fuel substrates and no adenylates,
 917 *i.e.*, AMP, ADP, ATP.

918 **State 2** is induced by addition of a ‘high’ concentration of ADP (typically 100 to 300
 919 μM), which stimulates respiration transiently on the basis of endogenous fuel substrates and
 920 phosphorylates only a small portion of the added ADP. State 2 is then obtained at a low
 921 respiratory activity limited by exhausted endogenous fuel substrate availability (**Table 3**). If
 922 addition of specific inhibitors of respiratory complexes—such as rotenone—does not cause a
 923 further decline of O₂ flux, State 2 is equivalent to the ROX state (See below.). If inhibition is

924 observed, undefined endogenous fuel substrates are a confounding factor of pathway control,
 925 contributing to the effect of subsequently externally added substrates and inhibitors. In contrast
 926 to the original protocol, an alternative sequence of titration steps is frequently applied, in which
 927 the alternative 'State 2' has an entirely different meaning, when this second state is induced by
 928 addition of fuel substrate without ADP or ATP (LEAK-state; in contrast to State 2 defined in
 929 **Table 1** as a ROX state). Some researchers have called this condition as "pseudostate 4"
 930 because it has no significant concentrations of adenine nucleotides and hence it is not a near-
 931 physiological condition, although it should be used for calculating the net OXPHOS-capacity,
 932 *P-L*.

933
 934 **Table 3. Metabolic states of mitochondria (Chance and**
 935 **Williams, 1956; Table V).**
 936

State	[O ₂]	ADP level	Substrate level	Respiration rate	Rate-limiting substance
1	>0	low	low	slow	ADP
2	>0	high	~0	slow	substrate
3	>0	high	high	fast	respiratory chain
4	>0	low	high	slow	ADP
5	0	high	high	0	oxygen

937
 938
 939 **State 3** is the state stimulated by addition of fuel substrates while the ADP concentration
 940 is still high (**Table 3**) and supports coupled energy transformation through oxidative
 941 phosphorylation. 'High ADP' is a concentration of ADP specifically selected to allow the
 942 measurement of State 3 to State 4 transitions of isolated mitochondria in a closed respirometric
 943 chamber. Repeated ADP titration re-establishes State 3 at 'high ADP'. Starting at O₂
 944 concentrations near air-saturation (193 or 238 μM O₂ at 37 °C or 25 °C and sea level at 1 atm
 945 or 101.32 kPa, and an oxygen solubility of respiration medium at 0.92 times that of pure water;
 946 Forstner and Gnaiger 1983), the total ADP concentration added must be low enough (typically
 947 100 to 300 μM) to allow phosphorylation to ATP at a coupled O₂ flux that does not lead to O₂
 948 depletion during the transition to State 4. In contrast, kinetically-saturating ADP concentrations
 949 usually are 10-fold higher than 'high ADP', *e.g.*, 2.5 mM in isolated mitochondria. The
 950 abbreviation State 3u is occasionally used in bioenergetics, to indicate the state of respiration
 951 after titration of an uncoupler, without sufficient emphasis on the fundamental difference
 952 between OXPHOS-capacity (*well-coupled* with an *endogenous* uncoupled component) and ET-
 953 capacity (*noncoupled*).

954 **State 4** is a LEAK-state that is obtained only if the mitochondrial preparation is intact
 955 and well-coupled. Depletion of ADP by phosphorylation to ATP causes a decline of O₂ flux in
 956 the transition from State 3 to State 4. Under the conditions of State 4, a maximum protonmotive
 957 force and high ATP/ADP ratio are maintained. The gradual decline of $Y_{P\gg O_2}$ towards
 958 diminishing [ADP] at State 4 must be taken into account for calculation of $P\gg O_2$ ratios (Gnaiger
 959 2001). State 4 respiration, L_T (**Table 1**), reflects intrinsic proton leak and ATP hydrolysis
 960 activity. O₂ flux in State 4 is an overestimation of LEAK-respiration if the contaminating ATP
 961 hydrolysis activity recycles some ATP to ADP, $J_{P\ll}$, which stimulates respiration coupled to
 962 phosphorylation, $J_{P\gg} > 0$. Some degree of mechanical disruption and loss of mitochondrial
 963 integrity allows the exposed mitochondrial F-ATPases to hydrolyze the ATP synthesized by
 964 the fraction of coupled mitochondria. This can be tested by inhibition of the phosphorylation-
 965 pathway using oligomycin, ensuring that $J_{P\gg} = 0$ (State 4o). On the other hand, the state 4
 966 respiration reached after exhaustion of added ADP is a more physiological condition (*i.e.*,
 967 presence of ATP, ADP and even AMP). Sequential ADP titrations re-establish State 3, followed

968 by State 3 to State 4 transitions while sufficient O₂ is available. Anoxia may be reached,
969 however, before exhaustion of ADP (State 5).

970 **State 5** is the state after exhaustion of O₂ in a closed respirometric chamber. Diffusion of
971 O₂ from the surroundings into the aqueous solution may be a confounding factor preventing
972 complete anoxia (Gnaiger 2001). Chance and Williams (1955) provide an alternative definition
973 of State 5, which gives it the different meaning of ROX versus anoxia: ‘State 5 may be obtained
974 by antimycin A treatment or by anaerobiosis’.

975 In **Table 3**, only States 3 and 4 are coupling control states, with the restriction that rates
976 in State 3 may be limited kinetically by non-saturating ADP concentrations.

977

978

979 3. What is a rate?

980

981 A rate may be considered as the numerator and normalization as the complementary
982 denominator, which are tightly linked in reporting the measurements in a format commensurate
983 with the requirements of a database. Application of common and defined units is required for
984 direct transfer of reported results into a database. The second [s] is the SI unit for the base
985 quantity *time*. It is also the standard time-unit used in solution chemical kinetics.

986 The term *rate* is not adequately defined to be useful for reporting data. The inconsistency
987 of the meanings of rate becomes apparent when considering Galileo Galilei’s famous principle,
988 that ‘bodies of different weight all fall at the same rate (have a constant acceleration)’
989 (Coopersmith 2010). A rate may be an extensive quantity, which is a *flow*, *I*, when expressed
990 per object (per number of cells or organisms) or per chamber (per system). ‘System’ is defined
991 as the open or closed chamber of the measuring device. A rate is a *flux*, *J*, when expressed as a
992 size-specific quantity (**Figure 7A; Box 2**).

993

994 • **Extensive quantities:** An extensive quantity increases proportionally with system
995 size. For example, mass and volume are extensive quantities. Flow is an extensive
996 quantity. The magnitude of an extensive quantity is completely additive for non-
997 interacting subsystems. The magnitude of these quantities depends on the extent or
998 size of the system (Cohen *et al.* 2008).

999 • **Size-specific quantities:** ‘The adjective *specific* before the name of an extensive
1000 quantity is often used to mean *divided by mass*’ (Cohen *et al.* 2008). In this system-
1001 paradigm, mass-specific flux is flow divided by mass of the *system* (the total mass of
1002 everything within the measuring chamber or reactor). Rates are frequently expressed
1003 as volume-specific flux. A mass-specific or volume-specific quantity is independent
1004 of the extent of non-interacting homogenous subsystems. Tissue-specific quantities
1005 (related to the *sample* in contrast to the *system*) are of fundamental interest in the field
1006 of comparative mitochondrial physiology, where *specific* refers to the *type of the*
1007 *sample* rather than *mass of the system*. The term *specific*, therefore, must be clarified;
1008 *sample-specific*, e.g., muscle mass-specific normalization, is distinguished from
1009 *system-specific* quantities (mass or volume; **Figure 7**).

1010 • **Intensive quantities:** In contrast to size-specific properties, forces are *intensive*
1011 quantities defined as the change of an extensive quantity per advancement of an
1012 energy transformation (Gnaiger 1993b).

1013

1014 N_X and m_X indicate the number format and mass format, respectively, for expressing the
1015 quantity of a sample *X*. When different formats are indicated in symbols of derived quantities,
1016 the format (\underline{N} , \underline{m}) is shown as a subscript (*underlined italic*), as in $I_{O_2/\underline{N}X}$ and $J_{O_2/\underline{m}X}$. Oxygen flow
1017 and flux are expressed in the molar format, n_{O_2} [mol], but in the volume format, V_{O_2} [m³] in

1018 ergometry. For mass-specific flux these formats can be distinguished as $J_{\underline{m}O_2/\underline{m}X}$ and $J_{\underline{V}O_2/\underline{m}X}$,
 1019 respectively. Further examples are given in **Figure 7** and **Table 4**.

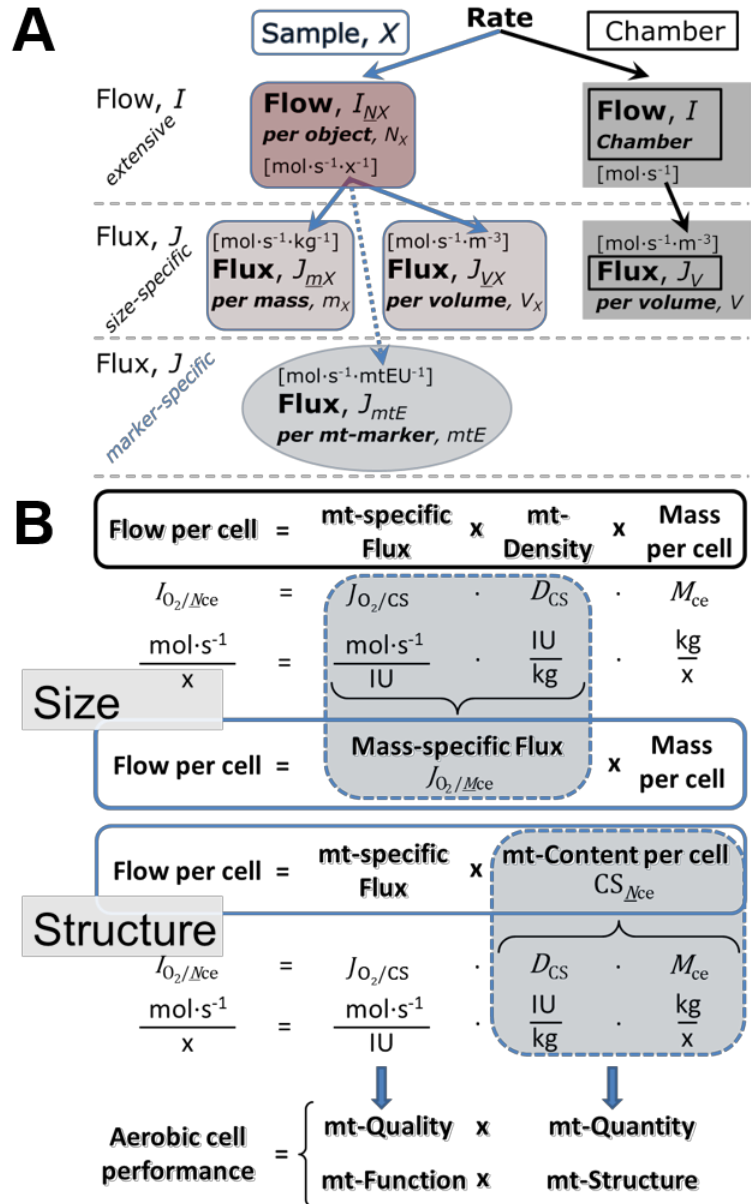
1020
1021

1022 **Figure 7. Flow and flux, and**
 1023 **normalization in structure-**
 1024 **function analysis**

1025 (A) When expressing metabolic
 1026 ‘rate’ measured in a chamber, a
 1027 fundamental distinction is made
 1028 between relating the rate to the
 1029 experimental sample (left) or
 1030 chamber (right). The different
 1031 meanings of rate need to be
 1032 specified by the chosen
 1033 normalization. Left: Results are
 1034 expressed as mass-specific *flux*,
 1035 J_{mX} , per mg protein, dry or wet
 1036 weight (mass). Cell volume, V_{ce} ,
 1037 may be used for normalization
 1038 (volume-specific flux, J_{Vce}).
 1039 Right: Flow per chamber, I , or
 1040 flux per chamber volume, J_V , are
 1041 merely reported for
 1042 methodological reasons.

1043 (B) O_2 flow per cell, $I_{O_2/Nce}$, is the
 1044 product of mitochondria-specific
 1045 flux, mt-density and mass per
 1046 cell. Unstructured analysis:
 1047 performance is the product of
 1048 mass-specific flux, $J_{O_2/MX}$
 1049 [$\text{mol}\cdot\text{s}^{-1}\cdot\text{kg}^{-1}$], and *size* (mass per
 1050 cell). Structured analysis:
 1051 performance is the product of
 1052 mitochondrial *function* (mt-
 1053 specific flux) and *structure* (mt-
 1054 content). Modified from Gnaiger
 1055 (2014). For further details see
 1056 **Table 4**.

1057
1058



1059 **Box 2: Metabolic flows and fluxes: vectoral, vectorial, and scalar**

1060
 1061 In a generalization of electrical terms, flow as an extensive quantity (I ; per system) is
 1062 distinguished from flux as a size-specific quantity (J ; per system size). *Flows*, I_{tr} , are defined
 1063 for all transformations as extensive quantities. Electric charge per unit time is electric flow or
 1064 current, $I_{el} = dQ_{el}\cdot dt^{-1}$ [$A \equiv C\cdot s^{-1}$]. When dividing I_{el} by size of the system (cross-sectional area
 1065 of a ‘wire’), we obtain flux as a size-specific quantity, which is the current density (surface-
 1066 density of flow) perpendicular to the direction of flux, $J_{el} = I_{el}\cdot A^{-1}$ [$A\cdot m^{-2}$] (Cohen et al. 2008).
 1067 Fluxes with *spatial* geometric direction and magnitude are *vectors*. Vector and scalar *fluxes* are
 1068 related to flows as $J_{tr} = I_{tr}\cdot A^{-1}$ [$\text{mol}\cdot\text{s}^{-1}\cdot\text{m}^{-2}$] and $J_{tr} = I_{tr}\cdot V^{-1}$ [$\text{mol}\cdot\text{s}^{-1}\cdot\text{m}^{-3}$], expressing flux as an
 1069 area-specific vector or volume-specific vectorial or scalar quantity, respectively (Gnaiger

1070 1993b). We use the metre–kilogram–second–ampere (MKSA) international system of units (*SI*)
 1071 for general cases ([m], [kg], [s] and [A]), with decimal *SI* prefixes for specific applications
 1072 (**Table 4**).

1073 We suggest to define: (1) *vectorial* fluxes, which are translocations as functions of
 1074 *gradients* with direction in geometric space in continuous systems; (2) *vectorial* fluxes, which
 1075 describe translocations in discontinuous systems and are restricted to information on
 1076 *compartmental differences* (**Figure 3**, transmembrane proton flux); and (3) *scalar* fluxes, which
 1077 are transformations in a *homogenous* system (**Figure 3**, catabolic O₂ flux, J_{kO_2}).

1078 Vectorial transmembrane proton fluxes, J_{mH^+pos} and J_{mH^+neg} , are analyzed in a
 1079 heterogenous compartmental system as a quantity with *directional* but not *spatial* information.
 1080 Translocation of protons across the mtIM has a defined direction, either from the negative
 1081 compartment (matrix space; negative, neg–compartment) to the positive compartment (inter-
 1082 membrane space; positive, pos–compartment) or *vice versa* (**Figure 3**). The arrows defining
 1083 the direction of the translocation between the two vesicular compartments may point upwards
 1084 or downwards, right or left, without any implication that these are actual directions in space.
 1085 The pos–compartment is neither above nor below the neg–compartment in a spatial sense, but
 1086 can be visualized arbitrarily in a figure in the upper position (**Figure 3**). In general, the
 1087 *compartmental direction* of vectorial translocation from the neg–compartment to the pos–
 1088 compartment is defined by assigning the initial and final state as *ergodynamic compartments*,
 1089 $H^+_{neg} \rightarrow H^+_{pos}$ or $0 = -1 H^+_{neg} + 1 H^+_{pos}$, related to work (erg = work) that must be performed to
 1090 lift the proton from a lower to a higher electrochemical potential or from the lower to the higher
 1091 ergodynamic compartment (Gnaiger 1993b).

1092 In analogy to *vectorial* translocation, the direction of a *scalar* chemical reaction, $A \rightarrow B$
 1093 or $0 = -1 A + 1 B$, is defined by assigning substrates and products, A and B, as ergodynamic
 1094 compartments. O₂ is defined as a substrate in respiratory O₂ consumption (electron acceptor),
 1095 which together with the fuel substrates (electron donors) comprises the substrate compartment
 1096 of the catabolic reaction. Volume-specific scalar O₂ flux is coupled to vectorial translocation,
 1097 yielding the H^+_{pos}/O_2 ratio (**Figure 2B**).

1098
 1099

1100 4. Normalization of rate per sample

1101

1102 The challenges of measuring mitochondrial respiratory flux are matched by those of
 1103 normalization. Normalization (**Table 4**) is guided by physicochemical principles,
 1104 methodological considerations, and conceptual strategies (**Figure 7**).

1105

1106 4.1. Flow: per object

1107

1108 **Number concentration, C_{NX} :** Normalization per sample concentration is routinely
 1109 required to report respiratory data. C_{NX} is the experimental *number concentration* of sample *X*.
 1110 In the case of animals, e.g., nematodes, $C_{NX} = N_X/V [x \cdot L^{-1}]$, where N_X is the number of organisms
 1111 in the chamber. Similarly, the number of cells per chamber volume is the number concentration
 1112 of permeabilized or intact cells $C_{Nce} = N_{ce}/V [x \cdot L^{-1}]$, where N_{ce} is the number of cells in the
 1113 chamber (**Table 4**).

1114 **Flow per object, $I_{O_2/NX}$:** O₂ flow per cell is calculated from volume-specific O₂ flux, J_{V,O_2}
 1115 [nmol·s⁻¹·L⁻¹] (per *V* of the measurement chamber [L]), divided by the number concentration of
 1116 cells. The total cell count is the sum of viable and dead cells, $N_{ce} = N_{vce} + N_{dce}$ (**Table 5**). The
 1117 cell viability index, $VI = N_{vce}/N_{ce}$, is the ratio of viable cells (N_{vce} ; before experimental
 1118 permeabilization) per total cell count. After experimental permeabilization, all cells are
 1119 permeabilized, $N_{pce} = N_{ce}$. The cell viability index can be used to normalize respiration for the
 1120 number of cells that have been viable before experimental permeabilization, $I_{O_2/Nvce} = I_{O_2/Nce}/VI$,

1121 considering that mitochondrial respiratory dysfunction in dead cells should be eliminated as a
 1122 confounding factor.

1123

1124
 1125

Table 4. Sample concentrations and normalization of flux.

Expression	Symbol	Definition	Unit	Notes
Sample				
identity of sample	X	object: cell, tissue, animal, patient		
number of sample entities X	N_X	number of objects	x	1
mass of sample X	m_X		kg	2
mass of object X	M_X	$M_X = m_X \cdot N_X^{-1}$	$\text{kg} \cdot \text{x}^{-1}$	2
Mitochondria				
Mitochondria	Mt	$X = \text{mt}$		
amount of mt-elementary components	mtE	quantity of mt-marker	mtEU	
Concentrations				
object number concentration	C_{NX}	$C_{NX} = N_X \cdot V^{-1}$	$\text{x} \cdot \text{m}^{-3}$	3
sample mass concentration	C_{mX}	$C_{mX} = m_X \cdot V^{-1}$	$\text{kg} \cdot \text{m}^{-3}$	
mitochondrial concentration	C_{mtE}	$C_{mtE} = mtE \cdot V^{-1}$	$\text{mtEU} \cdot \text{m}^{-3}$	4
specific mitochondrial density	D_{mtE}	$D_{mtE} = mtE \cdot m_X^{-1}$	$\text{mtEU} \cdot \text{kg}^{-1}$	5
mitochondrial content, mtE per object X	mtE_{NX}	$mtE_{NX} = mtE \cdot N_X^{-1}$	$\text{mtEU} \cdot \text{x}^{-1}$	6
O₂ flow and flux				
flow, system	I_{O_2}	internal flow	$\text{mol} \cdot \text{s}^{-1}$	7
volume-specific flux	J_{V,O_2}	$J_{V,O_2} = I_{O_2} \cdot V^{-1}$	$\text{mol} \cdot \text{s}^{-1} \cdot \text{m}^{-3}$	8
flow per object X	$I_{O_2/NX}$	$I_{O_2/NX} = J_{V,O_2} \cdot C_{NX}^{-1}$	$\text{mol} \cdot \text{s}^{-1} \cdot \text{x}^{-1}$	9
mass-specific flux	$J_{O_2/mX}$	$J_{O_2/mX} = J_{V,O_2} \cdot C_{mX}^{-1}$	$\text{mol} \cdot \text{s}^{-1} \cdot \text{kg}^{-1}$	10
mt-marker-specific flux	$J_{O_2/mtE}$	$J_{O_2/mtE} = J_{V,O_2} \cdot C_{mtE}^{-1}$	$\text{mol} \cdot \text{s}^{-1} \cdot \text{mtEU}^{-1}$	11

1126 1 The unit x for a number is not used by IUPAC. To avoid confusion, the units [$\text{kg} \cdot \text{x}^{-1}$] and [kg]
 1127 distinguish the mass per object from the mass of a sample that may contain any number of objects.
 1128 Similarly, the units for flow per system *versus* flow per object are [$\text{mol} \cdot \text{s}^{-1}$] (Note 8) and [$\text{mol} \cdot \text{s}^{-1} \cdot \text{x}^{-1}$]
 1129 (Note 10).

1130 2 Units are given in the MKSA system (**Box 2**). The *SI* prefix k is used for the *SI* base unit of mass (kg
 1131 = 1,000 g). In praxis, various *SI* prefixes are used for convenience, to make numbers easily readable,
 1132 e.g., 1 mg tissue, cell or mitochondrial mass instead of 0.000001 kg.

1133 3 In case of cells (sample $X = \text{cells}$), the object number concentration is $C_{N_{\text{ce}}} = N_{\text{ce}} \cdot V^{-1}$, and volume
 1134 may be expressed in [$\text{dm}^3 \equiv \text{L}$] or [$\text{cm}^3 = \text{mL}$]. See **Table 5** for different object types.

1135 4 mt-concentration is an experimental variable, dependent on sample concentration: (1) $C_{mtE} = mtE \cdot V^{-1}$;
 1136 (2) $C_{mtE} = mtE_X \cdot C_{NX}$; (3) $C_{mtE} = C_{mX} \cdot D_{mtE}$.

1137 5 If the amount of mitochondria, mtE , is expressed as mitochondrial mass, then D_{mtE} is the mass
 1138 fraction of mitochondria in the sample. If mtE is expressed as mitochondrial volume, V_{mt} , and the
 1139 mass of sample, m_X , is replaced by volume of sample, V_X , then D_{mtE} is the volume fraction of
 1140 mitochondria in the sample.

1141 6 $mtE_{NX} = mtE \cdot N_X^{-1} = C_{mtE} \cdot C_{NX}^{-1}$.

1142 7 O₂ can be replaced by other chemicals B to study different reactions, e.g., ATP, H₂O₂, or vesicular
 1143 compartmental translocations, e.g., Ca²⁺.

1144 8 I_{O_2} and V are defined per instrument chamber as a system of constant volume (and constant
 1145 temperature), which may be closed or open. I_{O_2} is abbreviated for I_{r,O_2} , i.e., the metabolic or internal
 1146 O₂ flow of the chemical reaction r in which O₂ is consumed, hence the negative stoichiometric
 1147 number, $\nu_{O_2} = -1$. $I_{r,O_2} = d_r n_{O_2} / dt \cdot \nu_{O_2}^{-1}$. If r includes all chemical reactions in which O₂ participates, then

- 1148 $d_i n_{O_2} = dn_{O_2} - d_e n_{O_2}$, where dn_{O_2} is the change in the amount of O_2 in the instrument chamber and $d_e n_{O_2}$
 1149 is the amount of O_2 added externally to the system. At steady state, by definition $dn_{O_2} = 0$, hence $d_i n_{O_2}$
 1150 $= -d_e n_{O_2}$.
- 1151 9 J_{V,O_2} is an experimental variable, expressed per volume of the instrument chamber.
- 1152 10 $I_{O_2/NX}$ is a physiological variable, depending on the size of entity X .
- 1153 11 There are many ways to normalize for a mitochondrial marker, that are used in different experimental
 1154 approaches: (1) $J_{O_2/mtE} = J_{V,O_2} \cdot C_{mtE}^{-1}$; (2) $J_{O_2/mtE} = J_{V,O_2} \cdot C_{mX}^{-1} \cdot D_{mtE}^{-1} = J_{O_2/mX} \cdot D_{mtE}^{-1}$; (3) $J_{O_2/mtE} =$
 1155 $J_{V,O_2} \cdot C_{NX}^{-1} \cdot mtE_{NX}^{-1} = I_{O_2/NX} \cdot mtE_{NX}^{-1}$; (4) $J_{O_2/mtE} = I_{O_2} \cdot mtE^{-1}$. The mt-elementary unit [mtEU] varies depending
 1156 on the mt-marker.
- 1157
 1158
 1159

Table 5. Sample types, X, abbreviations, and quantification.

Identity of sample	X	N_X	Mass ^a	Volume	mt-Marker
mitochondrial preparation		[x]	[kg]	[m ³]	[mtEU]
isolated mitochondria	imt		m_{mt}	V_{mt}	mtE
tissue homogenate	thom		m_{thom}		mtE_{thom}
permeabilized tissue	pti		m_{pti}		mtE_{pti}
permeabilized fibre	pfi		m_{pfi}		mtE_{pfi}
permeabilized cell	pce	N_{pce}	M_{pce}	V_{pce}	mtE_{pce}
cells ^b	ce	N_{ce}	M_{ce}	V_{ce}	mtE_{ce}
intact cell, viable cell	vce	N_{vce}	M_{vce}	V_{vce}	
dead cell	dce	N_{dce}	M_{dce}	V_{dce}	
organism	org	N_{org}	M_{org}	V_{org}	

1160 ^a Instead of mass, the wet weight or dry weight is frequently stated, W_w or W_d .
 1161 m_X is mass of the sample [kg], M_X is mass of the object [kg·x⁻¹] (Table 4).

1162 ^b Total cell count, $N_{ce} = N_{vce} + N_{dce}$

1163

1164 The complexity changes when the sample is a whole organism studied as an experimental
 1165 model. The scaling law in respiratory physiology reveals a strong interaction between O_2 flow
 1166 and individual body mass, since *basal* metabolic rate (flow) does not increase linearly with
 1167 body mass, whereas *maximum* mass-specific O_2 flux, \dot{V}_{O_2max} or \dot{V}_{O_2peak} , is approximately
 1168 constant across a large range of individual body mass (Weibel and Hoppeler 2005), with
 1169 individuals, breeds, and species deviating substantially from this relationship. \dot{V}_{O_2peak} of human
 1170 endurance athletes is 60 to 80 mL $O_2 \cdot \text{min}^{-1} \cdot \text{kg}^{-1}$ body mass, converted to $J_{O_2peak/Morg}$ of 45 to 60
 1171 nmol·s⁻¹·g⁻¹ (Gnaiger 2014; Table 6).

1172

1173 4.2. Size-specific flux: per sample size

1174

1175 **Sample concentration, C_{mX} :** Considering permeabilized tissue, homogenate or cells as
 1176 the sample, X , the sample mass is m_X [mg], which is frequently measured as wet or dry weight,
 1177 W_w or W_d [mg], respectively, or as amount of protein, $m_{Protein}$. The sample concentration is the
 1178 mass of the subsample per volume of the measurement chamber, $C_{mX} = m_X/V$ [g·L⁻¹ = mg·mL⁻¹].
 1179 X is the type of sample—isolated mitochondria, tissue homogenate, permeabilized fibres or
 1180 cells (Table 5).

1181 **Size-specific flux:** Cellular O_2 flow can be compared between cells of identical size. To
 1182 take into account changes and differences in cell size, normalization is required to obtain cell
 1183 size-specific or mitochondrial marker-specific O_2 flux (Renner *et al.* 2003).

- 1184 • **Mass-specific flux, $J_{O_2/mX}$** [mol·s⁻¹·kg⁻³]: Mass-specific flux is obtained by expressing
 1185 respiration per mass of sample, m_X [mg]. Flow per cell is divided by mass per cell,

1186 $J_{O_2/mce} = I_{O_2/Nce}/M_{Nce}$. Or chamber volume-specific flux, J_{V,O_2} , is divided by mass
 1187 concentration of X in the chamber, $J_{O_2/mX} = J_{V,O_2}/C_{mX}$.

1188 • **Cell volume-specific flux, $J_{O_2/VX}$ [$\text{mol}\cdot\text{s}^{-1}\cdot\text{m}^{-3}$]**: Sample volume-specific flux is
 1189 obtained by expressing respiration per volume of sample. For example, in the case of
 1190 using cells as sample will be the volume of cells added to the chamber (**Figure 7**).
 1191

1192 If size-specific O_2 flux is constant and independent of sample size, then there is no
 1193 interaction between the subsystems. For example, a 1.5 mg and a 3.0 mg muscle sample respire
 1194 at identical mass-specific flux. Mass-specific O_2 flux, however, may change with the mass of a
 1195 tissue sample, cells or isolated mitochondria in the measuring chamber, in which the nature of
 1196 the interaction becomes an issue. Therefore, cell density must be optimized, particularly in
 1197 experiments carried out in wells, considering the confluency of the cell monolayer or clumps
 1198 of cells (Salabei *et al.* 2014).
 1199

1200 4.3. Marker-specific flux: per mitochondrial content

1201
 1202 Tissues can contain multiple cell populations that may have distinct mitochondrial
 1203 subtypes. Mitochondria undergo dynamic fission and fusion cycles, and can exist in multiple
 1204 stages and sizes that may be altered by a range of factors. The isolation of mitochondria (often
 1205 achieved through differential centrifugation) can therefore yield a subsample of the
 1206 mitochondrial types present in a tissue, depending on the isolation protocols utilized (*e.g.*,
 1207 centrifugation speed). This possible bias should be taken into account when planning
 1208 experiments using isolated mitochondria. Different sizes of mitochondria are enriched at
 1209 specific centrifugation speeds, which can be used strategically for isolation of mitochondrial
 1210 subpopulations.

1211 Part of the mitochondrial content of a tissue is lost during preparation of isolated
 1212 mitochondria. The fraction of isolated mitochondria obtained from a tissue sample is expressed
 1213 as mitochondrial recovery. At a high mitochondrial recovery the fraction of isolated
 1214 mitochondria is more representative of the total mitochondrial population than in preparations
 1215 characterized by low recovery. Determination of the mitochondrial recovery and yield is based
 1216 on measurement of the concentration of a mitochondrial marker in the stock of isolated
 1217 mitochondria, $C_{mtE,stock}$, and crude tissue homogenate, $C_{mtE,thom}$, which simultaneously provides
 1218 information on the specific mitochondrial density in the sample, D_{mtE} (**Table 4**).
 1219

1220 Normalization is a problematic subject; it is essential to consider the question of the study.
 1221 If the study aims at comparing tissue performance—such as the effects of a treatment on a
 1222 specific tissue, then normalization for tissue mass or protein content is appropriate. However,
 1223 if the aim is to find differences on mitochondrial function independent of mitochondrial density
 1224 (**Table 4**), then normalization to a mitochondrial marker is imperative (**Figure 7**). One cannot
 1225 assume that quantitative changes in various markers—such as mitochondrial proteins—
 1226 necessarily occur in parallel with one another. It should be established that the marker chosen
 1227 is not selectively altered by the performed treatment. In conclusion, the normalization must
 1228 reflect the question under investigation to reach a satisfying answer. On the other hand, the goal
 1229 of comparing results across projects and institutions requires standardization on normalization
 for entry into a databank.

1230 **Mitochondrial concentration, C_{mtE} , and mitochondrial markers:** Mitochondrial
 1231 organelles comprise a dynamic cellular reticulum in various states of fusion and fission. Hence,
 1232 the definition of an "amount" of mitochondria is often misconceived: mitochondria cannot be
 1233 counted reliably as a number of occurring elementary components. Therefore, quantification of
 1234 the "amount" of mitochondria depends on the measurement of chosen mitochondrial markers.
 1235 'Mitochondria are the structural and functional elementary units of cell respiration' (Gnaiger
 1236 2014). The quantity of a mitochondrial marker can reflect the amount of *mitochondrial*

1237 *elementary components, mtE*, expressed in various mitochondrial elementary units [mtEU]
 1238 specific for each measured mt-marker (**Table 4**). However, since mitochondrial quality may
 1239 change in response to stimuli—particularly in mitochondrial dysfunction (Campos *et al.* 2017)
 1240 and after exercise training (Pesta *et al.* 2011) and during aging (Daum *et al.* 2013)—some
 1241 markers can vary while others are unchanged: (1) Mitochondrial volume and membrane area
 1242 are structural markers, whereas mitochondrial protein mass is frequently used as a marker for
 1243 isolated mitochondria. (2) Molecular and enzymatic mitochondrial markers (amounts or
 1244 activities) can be selected as matrix markers, *e.g.*, citrate synthase activity, mtDNA; mtIM-
 1245 markers, *e.g.*, cytochrome *c* oxidase activity, *aa3* content, cardiolipin, or mtOM-markers, *e.g.*,
 1246 the voltage-dependent anion channel (VDAC), TOM20. (3) Extending the measurement of
 1247 mitochondrial marker enzyme activity to mitochondrial pathway capacity, ET- or OXPHOS-
 1248 capacity can be considered as an integrative functional mitochondrial marker.

1249 Depending on the type of mitochondrial marker, the mitochondrial elementary
 1250 component, *mtE*, is expressed in marker-specific units. Mitochondrial concentration in the
 1251 measurement chamber and the tissue of origin are quantified as (1) a quantity for normalization
 1252 in functional analyses, C_{mtE} , and (2) a physiological output that is the result of mitochondrial
 1253 biogenesis and degradation, D_{mtE} , respectively (**Table 4**). It is recommended, therefore, to
 1254 distinguish *experimental mitochondrial concentration*, $C_{mtE} = mtE/V$ and *physiological*
 1255 *mitochondrial density*, $D_{mtE} = mtE/m_X$. Then mitochondrial density is the amount of
 1256 mitochondrial elementary components per mass of tissue, which is a biological variable (**Figure**
 1257 **7**). The experimental variable is mitochondrial density multiplied by sample mass concentration
 1258 in the measuring chamber, $C_{mtE} = D_{mtE} \cdot C_{m_X}$, or mitochondrial content multiplied by sample
 1259 number concentration, $C_{mtE} = mtE_X \cdot C_{NX}$ (**Table 4**).

1260 **mt-Marker-specific flux, $J_{O_2/mtE}$** : Volume-specific metabolic O_2 flux depends on: (1) the
 1261 sample concentration in the volume of the instrument chamber, C_{m_X} , or C_{NX} ; (2) the
 1262 mitochondrial density in the sample, $D_{mtE} = mtE/m_X$ or $mtE_X = mtE/N_X$; and (3) the specific
 1263 mitochondrial activity or performance per elementary mitochondrial unit, $J_{O_2/mtE} = J_{V,O_2}/C_{mtE}$
 1264 [$\text{mol} \cdot \text{s}^{-1} \cdot \text{mtEU}^{-1}$] (**Table 4**). Obviously, the numerical results for $J_{O_2/mtE}$ vary with the type of
 1265 mitochondrial marker chosen for measurement of *mtE* and $C_{mtE} = mtE/V$ [$\text{mtEU} \cdot \text{m}^{-3}$].

1266 Different methods are implicated in the quantification of mitochondrial markers and have
 1267 different strengths. Some problems are common for all mitochondrial markers, *mtE*: (1)
 1268 Accuracy of measurement is crucial, since even a highly accurate and reproducible
 1269 measurement of O_2 flux results in an inaccurate and noisy expression if normalized by a biased
 1270 and noisy measurement of a mitochondrial marker. This problem is acute in mitochondrial
 1271 respiration because the denominators used (the mitochondrial markers) are often small moieties
 1272 of which accurate and precise determination is difficult. This problem can be avoided when O_2
 1273 fluxes measured in substrate-uncoupler-inhibitor titration protocols are normalized for flux in
 1274 a defined respiratory reference state, which is used as an *internal* marker and yields flux control
 1275 ratios, *FCRs*. *FCRs* are independent of *externally* measured markers and, therefore, are
 1276 statistically robust, considering the limitations of ratios in general (Jasienski and Bazzaz 1999).
 1277 *FCRs* indicate qualitative changes of mitochondrial respiratory control, with highest
 1278 quantitative resolution, separating the effect of mitochondrial density or concentration on J_{O_2/m_X}
 1279 and I_{O_2/N_X} from that of function per elementary mitochondrial marker, $J_{O_2/mtE}$ (Pesta *et al.* 2011;
 1280 Gnaiger 2014). (2) If mitochondrial quality does not change and only the amount of
 1281 mitochondria varies as a determinant of mass-specific flux, any marker is equally qualified in
 1282 principle; then in practice selection of the optimum marker depends only on the accuracy and
 1283 precision of measurement of the mitochondrial marker. (3) If mitochondrial flux control ratios
 1284 change, then there may not be any best mitochondrial marker. In general, measurement of
 1285 multiple mitochondrial markers enables a comparison and evaluation of normalization for a
 1286 variety of mitochondrial markers. Particularly during postnatal development, the activity of
 1287 marker enzymes—such as cytochrome *c* oxidase and citrate synthase—follows different time

1288 courses (Drahota *et al.* 2004). Evaluation of mitochondrial markers in healthy controls is
 1289 insufficient for providing guidelines for application in the diagnosis of pathological states and
 1290 specific treatments.

1291 In line with the concept of the respiratory control ratio (Chance and Williams 1955a), the
 1292 most readily used normalization is that of flux control ratios and flux control factors (Gnaiger
 1293 2014). Selection of the state of maximum flux in a protocol as the reference state has the
 1294 advantages of: (1) internal normalization; (2) statistically validated linearization of the response
 1295 in the range of 0 to 1; and (3) consideration of maximum flux for integrating a large number of
 1296 elementary steps in the OXPHOS- or ET-pathways. This reduces the risk of selecting a
 1297 functional marker that is specifically altered by the treatment or pathology, yet increases the
 1298 chance that the highly integrative pathway is disproportionately affected, *e.g.*, the OXPHOS-
 1299 rather than ET-pathway in case of an enzymatic defect in the phosphorylation-pathway. In this
 1300 case, additional information can be obtained by reporting flux control ratios based on a
 1301 reference state which indicates stable tissue-mass specific flux.

1302 Stereological determination of mitochondrial content via two-dimensional transmission
 1303 electron microscopy can have limitations due to the dynamics of mitochondrial size (Meinild
 1304 Lundby *et al.* 2017). Accurate determination of three-dimensional volume by two-dimensional
 1305 microscopy can be both time consuming and statistically challenging (Larsen *et al.* 2012).

1306 The validity of using mitochondrial marker enzymes (citrate synthase activity, CI to CIV
 1307 amount or activity) for normalization of flux is limited in part by the same factors that apply to
 1308 flux control ratios. Strong correlations between various mitochondrial markers and citrate
 1309 synthase activity (Reichmann *et al.* 1985; Boushel *et al.* 2007; Mogensen *et al.* 2007) are
 1310 expected in a specific tissue of healthy persons and in disease states not specifically targeting
 1311 citrate synthase. Citrate synthase activity is acutely modifiable by exercise (Tonkonogi *et al.*
 1312 1997; Leek *et al.* 2001). Evaluation of mitochondrial markers related to a selected age and sex
 1313 cohort cannot be extrapolated to provide recommendations for normalization in respirometric
 1314 diagnosis of disease, in different states of development and ageing, different cell types, tissues,
 1315 and species. mtDNA normalized to nDNA via qPCR is correlated to functional mitochondrial
 1316 markers including OXPHOS- and ET-capacity in some cases (Puntschart *et al.* 1995; Wang *et al.*
 1317 1999; Menshikova *et al.* 2006; Boushel *et al.* 2007; Ehinger *et al.* 2015), but lack of such
 1318 correlations have been reported (Menshikova *et al.* 2005; Schultz and Wiesner 2000; Pesta *et al.*
 1319 2011). Several studies indicate a strong correlation between cardiolipin content and increase
 1320 in mitochondrial function with exercise (Menshikova *et al.* 2005; Menshikova *et al.* 2007;
 1321 Larsen *et al.* 2012; Faber *et al.* 2014), but it has not been evaluated as a general mitochondrial
 1322 biomarker in disease. With no single best mitochondrial marker, a good strategy is to quantify
 1323 several different biomarkers to minimize the decorrelating effects caused by diseases,
 1324 treatments, or other factors. Determination of multiple markers, particularly a matrix marker
 1325 and a marker from the mtIM, allows tracking changes in mitochondrial quality defined by their
 1326 ratio.

1327

1328

1329 **5. Normalization of rate per system**

1330

1331 *5.1. Flow: per chamber*

1332

1333 The experimental system (experimental chamber) is part of the measurement instrument,
 1334 separated from the environment as an isolated, closed, open, isothermal or non-isothermal
 1335 system (**Table 4**). Reporting O₂ flows per respiratory chamber, I_{O_2} [nmol·s⁻¹], restricts the
 1336 analysis to intra-experimental comparison of relative differences.

1337

1338

5.2. Flux: per chamber volume

System-specific flux, J_{V,O_2} : We distinguish between (1) the *system* with volume V and mass m defined by the system boundaries, and (2) the *sample* or *objects* with volume V_X and mass m_X that are enclosed in the experimental chamber (Figure 7). Metabolic O_2 flow per object, I_{O_2/N_X} , is the total O_2 flow in the system divided by the number of objects, N_X , in the system. I_{O_2/N_X} increases as the mass of the object is increased. Sample mass-specific O_2 flux, J_{O_2/m_X} should be independent of the mass of the sample studied in the instrument chamber, but system volume-specific O_2 flux, J_{V,O_2} (per volume of the instrument chamber), increases in proportion to the mass of the sample in the chamber. Whereas J_{V,O_2} depends on mass-concentration of the sample in the chamber, it should be independent of the chamber (system) volume at constant sample mass. There are practical limitations to increase the mass-concentration of the sample in the chamber, when one is concerned about crowding effects and instrumental time resolution.

Advancement per volume: When the reactor volume does not change during the reaction, which is typical for liquid phase reactions, the volume-specific flux of a chemical reaction r is the time derivative of the advancement of the reaction per unit volume, $J_{V,rB} = d_{t,r} \xi_B / dt \cdot V^{-1}$ [(mol·s⁻¹)·L⁻¹]. The rate of concentration change is dc_B/dt [(mol·L⁻¹)·s⁻¹], where concentration is $c_B = n_B/V$. There is a difference between (1) J_{V,rO_2} [mol·s⁻¹·L⁻¹] and (2) rate of concentration change [mol·L⁻¹·s⁻¹]. These merge to a single expression only in closed systems. In open systems, external fluxes (such as O_2 supply) are distinguished from internal transformations (catabolic flux, O_2 consumption). In a closed system, external flows of all substances are zero and O_2 consumption (internal flow of catabolic reactions k), I_{kO_2} [pmol·s⁻¹], causes a decline of the amount of O_2 in the system, n_{O_2} [nmol]. Normalization of these quantities for the volume of the system, V [L \equiv dm³], yields volume-specific O_2 flux, $J_{V,kO_2} = I_{kO_2}/V$ [nmol·s⁻¹·L⁻¹], and O_2 concentration, $[O_2]$ or $c_{O_2} = n_{O_2}/V$ [μ mol·L⁻¹ = μ M = nmol·mL⁻¹]. Instrumental background O_2 flux is due to external flux into a non-ideal closed respirometer; then total volume-specific flux has to be corrected for instrumental background O_2 flux— O_2 diffusion into or out of the instrumental chamber. J_{V,kO_2} is relevant mainly for methodological reasons and should be compared with the accuracy of instrumental resolution of background-corrected flux, e.g., ± 1 nmol·s⁻¹·L⁻¹ (Gnaiger 2001). ‘Metabolic’ or catabolic indicates O_2 flux, J_{kO_2} , corrected for: (1) instrumental background O_2 flux; (2) chemical background O_2 flux due to autoxidation of chemical components added to the incubation medium; and (3) *Rox* for O_2 -consuming side reactions unrelated to the catabolic pathway k .

6. Conversion of units

Many different units have been used to report the O_2 consumption rate, OCR (Table 6). *SI* base units provide the common reference to introduce the theoretical principles (Figure 7), and are used with appropriately chosen *SI* prefixes to express numerical data in the most practical format, with an effort towards unification within specific areas of application (Table 7). Reporting data in *SI* units—including the mole [mol], coulomb [C], joule [J], and second [s]—should be encouraged, particularly by journals which propose the use of *SI* units.

Although volume is expressed as m³ using the *SI* base unit, the litre [dm³] is a conventional unit of volume for concentration and is used for most solution chemical kinetics. If one multiplies $I_{O_2/N_{ce}}$ by $C_{N_{ce}}$, then the result will not only be the amount of O_2 [mol] consumed per time [s⁻¹] in one litre [L⁻¹], but also the change in O_2 concentration per second (for any volume of an ideally closed system). This is ideal for kinetic modeling as it blends with chemical rate equations where concentrations are typically expressed in mol·L⁻¹ (Wagner *et al.* 2011). In studies of multinuclear cells—such as differentiated skeletal muscle cells—it is easy

1390 to determine the number of nuclei but not the total number of cells. A generalized concept,
 1391 therefore, is obtained by substituting cells by nuclei as the sample entity. This does not hold,
 1392 however, for enucleated platelets.

1393

1394 **Table 6. Conversion of various formats and units used in respirometry and**
 1395 **ergometry.** e^- is the number of electrons or reducing equivalents. z_B is the charge
 1396 number of entity B.

Format	1 Unit		Multiplication factor	SI-unit	Notes
\underline{n}	ng.atom O \cdot s $^{-1}$	(2 e^-)	0.5	nmol O $_2$ \cdot s $^{-1}$	
\underline{n}	ng.atom O \cdot min $^{-1}$	(2 e^-)	8.33	pmol O $_2$ \cdot s $^{-1}$	
\underline{n}	natom O \cdot min $^{-1}$	(2 e^-)	8.33	pmol O $_2$ \cdot s $^{-1}$	
\underline{n}	nmol O $_2$ \cdot min $^{-1}$	(4 e^-)	16.67	pmol O $_2$ \cdot s $^{-1}$	
\underline{n}	nmol O $_2$ \cdot h $^{-1}$	(4 e^-)	0.2778	pmol O $_2$ \cdot s $^{-1}$	
\underline{V} to \underline{n}	mL O $_2$ \cdot min $^{-1}$ at STPD a		0.744	μ mol O $_2$ \cdot s $^{-1}$	1
\underline{e} to \underline{n}	W = J/s at -470 kJ/mol O $_2$		-2.128	μ mol O $_2$ \cdot s $^{-1}$	
\underline{e} to \underline{n}	mA = mC \cdot s $^{-1}$	($z_{H^+} = 1$)	10.36	nmol H $^+$ \cdot s $^{-1}$	2
\underline{e} to \underline{n}	mA = mC \cdot s $^{-1}$	($z_{O_2} = 4$)	2.59	nmol O $_2$ \cdot s $^{-1}$	2
\underline{n} to \underline{e}	nmol H $^+$ \cdot s $^{-1}$	($z_{H^+} = 1$)	0.09649	mA	3
\underline{n} to \underline{e}	nmol O $_2$ \cdot s $^{-1}$	($z_{O_2} = 4$)	0.38594	mA	3

1398 1 At standard temperature and pressure dry (STPD: 0 °C = 273.15 K and 1 atm = 101.325
 1399 kPa = 760 mmHg), the molar volume of an ideal gas, V_m , and V_{m,O_2} is 22.414 and 22.392
 1400 L \cdot mol $^{-1}$, respectively. Rounded to three decimal places, both values yield the conversion
 1401 factor of 0.744. For comparison at normal temperature and pressure dry (NTPD: 20 °C),
 1402 V_{m,O_2} is 24.038 L \cdot mol $^{-1}$. Note that the SI standard pressure is 100 kPa.

1403 2 The multiplication factor is $10^6/(z_B \cdot F)$.

1404 3 The multiplication factor is $z_B \cdot F/10^6$.

1405

1406 For studies of cells, we recommend that respiration be expressed, as far as possible, as:
 1407 (1) O $_2$ flux normalized for a mitochondrial marker, for separation of the effects of mitochondrial
 1408 quality and content on cell respiration (this includes $FCRs$ as a normalization for a functional
 1409 mitochondrial marker); (2) O $_2$ flux in units of cell volume or mass, for comparison of respiration
 1410 of cells with different cell size (Renner *et al.* 2003) and with studies on tissue preparations, and
 1411 (3) O $_2$ flow in units of attomole (10^{-18} mol) of O $_2$ consumed in a second by each cell
 1412 [amol \cdot s $^{-1}$ \cdot cell $^{-1}$], numerically equivalent to [pmol \cdot s $^{-1}$ \cdot 10 $^{-6}$ cells]. This convention allows
 1413 information to be easily used when designing experiments in which O $_2$ flow must be considered.
 1414 For example, to estimate the volume-specific O $_2$ flux in an instrument chamber that would be
 1415 expected at a particular cell number concentration, one simply needs to multiply the flow per
 1416 cell by the number of cells per volume of interest. This provides the amount of O $_2$ [mol]
 1417 consumed per time [s $^{-1}$] per unit volume [L $^{-1}$]. At an O $_2$ flow of 100 amol \cdot s $^{-1}$ \cdot cell $^{-1}$ and a cell
 1418 density of 10 9 cells \cdot L $^{-1}$ (10 6 cells \cdot mL $^{-1}$), the volume-specific O $_2$ flux is 100 nmol \cdot s $^{-1}$ \cdot L $^{-1}$ (100
 1419 pmol \cdot s $^{-1}$ \cdot mL $^{-1}$).

1420 ET-capacity in human cell types including HEK 293, primary HUVEC and fibroblasts
 1421 ranges from 50 to 180 amol \cdot s $^{-1}$ \cdot cell $^{-1}$, measured in intact cells in the noncoupled state (see
 1422 Gnaiger 2014). At 100 amol \cdot s $^{-1}$ \cdot cell $^{-1}$ corrected for Rox , the current across the mt-membranes,
 1423 I_{H^+e} , approximates 193 pA \cdot cell $^{-1}$ or 0.2 nA per cell. See Rich (2003) for an extension of
 1424 quantitative bioenergetics from the molecular to the human scale, with a transmembrane proton
 1425 flux equivalent to 520 A in an adult at a catabolic power of -110 W. Modelling approaches
 1426 illustrate the link between protonmotive force and currents (Willis *et al.* 2016).

1427 **Table 7. Conversion of units with preservation of numerical values.**

Name	Frequently used unit	Equivalent unit	Notes
volume-specific flux, J_{V,O_2}	$\text{pmol}\cdot\text{s}^{-1}\cdot\text{mL}^{-1}$ $\text{mmol}\cdot\text{s}^{-1}\cdot\text{L}^{-1}$	$\text{nmol}\cdot\text{s}^{-1}\cdot\text{L}^{-1}$ $\text{mol}\cdot\text{s}^{-1}\cdot\text{m}^{-3}$	1
cell-specific flow, $I_{O_2/\text{cell}}$	$\text{pmol}\cdot\text{s}^{-1}\cdot 10^{-6}$ cells	$\text{amol}\cdot\text{s}^{-1}\cdot\text{cell}^{-1}$	2
	$\text{pmol}\cdot\text{s}^{-1}\cdot 10^{-9}$ cells	$\text{zmol}\cdot\text{s}^{-1}\cdot\text{cell}^{-1}$	3
cell number concentration, C_{Nce}	10^6 cells $\cdot\text{mL}^{-1}$	10^9 cells $\cdot\text{L}^{-1}$	
mitochondrial protein concentration, C_{mtE}	0.1 mg $\cdot\text{mL}^{-1}$	0.1 g $\cdot\text{L}^{-1}$	
mass-specific flux, $J_{O_2/m}$	$\text{pmol}\cdot\text{s}^{-1}\cdot\text{mg}^{-1}$	$\text{nmol}\cdot\text{s}^{-1}\cdot\text{g}^{-1}$	4
catabolic power, P_k	$\mu\text{W}\cdot 10^{-6}$ cells	$\text{pW}\cdot\text{cell}^{-1}$	1
Volume	1,000 L	m^3 (1,000 kg)	
	L	dm^3 (kg)	
	mL	cm^3 (g)	
	μL	mm^3 (mg)	
	fL	μm^3 (pg)	5
amount of substance concentration	$\text{M} = \text{mol}\cdot\text{L}^{-1}$	$\text{mol}\cdot\text{dm}^{-3}$	

1428

1429 1 pmol: picomole = 10^{-12} mol1430 2 amol: attomole = 10^{-18} mol1431 3 zmol: zeptomole = 10^{-21} mol

1432

1433 We consider isolated mitochondria as powerhouses and proton pumps as molecular
 1434 machines to relate experimental results to energy metabolism of the intact cell. The cellular
 1435 P_{\gg}/O_2 based on oxidation of glycogen is increased by the glycolytic (fermentative) substrate-
 1436 level phosphorylation of 3 P_{\gg}/Glyc or 0.5 mol P_{\gg} for each mol O_2 consumed in the complete
 1437 oxidation of a mol glycosyl unit (Glyc). Adding 0.5 to the mitochondrial P_{\gg}/O_2 ratio of 5.4
 1438 yields a bioenergetic cell physiological P_{\gg}/O_2 ratio close to 6. Two NADH equivalents are
 1439 formed during glycolysis and transported from the cytosol into the mitochondrial matrix, either
 1440 by the malate-aspartate shuttle or by the glycerophosphate shuttle (**Figure 2A**) resulting in
 1441 different theoretical yields of ATP generated by mitochondria, the energetic cost of which
 1442 potentially must be taken into account. Considering also substrate-level phosphorylation in the
 1443 TCA cycle, this high P_{\gg}/O_2 ratio not only reflects proton translocation and OXPHOS studied
 1444 in isolation, but integrates mitochondrial physiology with energy transformation in the living
 1445 cell (Gnaiger 1993a).

1446

1447

1448 **7. Conclusions**

1449

1450 Catabolic cell respiration is the process of exergonic and exothermic energy
 1451 transformation in which scalar redox reactions are coupled to vectorial ion translocation across
 1452 a semipermeable membrane, which separates the small volume of a bacterial cell or
 1453 mitochondrion from the larger volume of its surroundings. The electrochemical exergy can be
 1454 partially conserved in the phosphorylation of ADP to ATP or in ion pumping, or dissipated in
 1455 an electrochemical short-circuit. Respiration is thus clearly distinguished from fermentation as
 1456 the counterpart of cellular core energy metabolism. An O_2 flux balance scheme illustrates the
 1457 relationships and general definitions (**Figures 1 and 2**).

1458 Experimentally, respiration is separated in mitochondrial preparations from the
 1459 interactions with the fermentative pathways of the intact cell. OXPHOS analysis (**Figure 3**) is
 1460 based on the study of mitochondrial preparations complementary to bioenergetic investigations

1461 of intact cells and organisms—from model organisms to the human species including healthy
 1462 and diseased persons (patients). Different mechanisms of respiratory uncoupling have to be
 1463 distinguished (**Figure 4**). Metabolic fluxes measured in defined coupling and pathway control
 1464 states (**Figures 5 and 6**) provide insights into the meaning of cellular and organismic
 1465 respiration.

1466 The optimal choice for expressing mitochondrial and cell respiration as O₂ flow per
 1467 biological sample, and normalization for specific tissue-markers (volume, mass, protein) and
 1468 mitochondrial markers (volume, protein, content, mtDNA, activity of marker enzymes,
 1469 respiratory reference state) is guided by the scientific question under study. Interpretation of
 1470 the data depends critically on appropriate normalization (**Figure 7**).

1471 MitoEAGLE can serve as a gateway to better diagnose mitochondrial respiratory
 1472 adaptations and defects linked to genetic variation, age-related health risks, sex-specific
 1473 mitochondrial performance, lifestyle with its effects on degenerative diseases, and thermal and
 1474 chemical environment. The present recommendations on coupling control states and rates,
 1475 linked to the concept of the protonmotive force, are focused on studies with mitochondrial
 1476 preparations (**Box 3**). These will be extended in a series of reports on pathway control of
 1477 mitochondrial respiration, respiratory states in intact cells, and harmonization of experimental
 1478 procedures.

1479

1480 **Box 3: Recommendations for studies with mitochondrial preparations**

1481

- 1482 ● Normalization of respiratory rates should be provided as far as possible:

1483 1. *Biophysical normalization*: on a per cell basis as O₂ flow; this may not be possible
 1484 when dealing with coenocytic organisms or tissues without cross-walls
 1485 separating individual cells (e.g., filamentous fungi, muscle fibers)

1486 2. *Cellular normalization*: per g protein; per cell- or tissue-mass as mass-specific
 1487 O₂ flux; per cell volume as cell volume-specific flux

1488 3. *Mitochondrial normalization*: per mitochondrial marker as mt-specific flux.

1489 With information on cell size and the use of multiple normalizations, maximum potential
 1490 information is available (Renner *et al.* 2003; Wagner *et al.* 2011; Gnaiger 2014). Reporting
 1491 flow in a respiratory chamber [nmol·s⁻¹] is discouraged, since it restricts the analysis to intra-
 1492 experimental comparison of relative (qualitative) differences.

- 1493 ● Catabolic mitochondrial respiration is distinguished from residual O₂ consumption. Fluxes
 1494 in mitochondrial coupling states should be, as far as possible, corrected for residual O₂
 1495 consumption.

- 1496 ● Different mechanisms of uncoupling should be distinguished by defined terms. The tightness
 1497 of coupling relates to these uncoupling mechanisms, whereas the coupling stoichiometry
 1498 varies as a function the substrate type involved in ET-pathways with either three or two
 1499 redox proton pumps operating in series. Separation of tightness of coupling from the
 1500 pathway-dependent coupling stoichiometry is possible only when the substrate type
 1501 undergoing oxidation remains the same for respiration in LEAK-, OXPHOS-, and ET-states.
 1502 In studies of the tightness of coupling, therefore, simple substrate-inhibitor combinations
 1503 should be applied to exclude a shift in substrate competition which may occur when
 1504 providing physiological substrate cocktails.

- 1505 ● In studies of isolated mitochondria, the mitochondrial recovery and yield should be reported.
 1506 Experimental criteria for evaluation of purity versus integrity should be considered.
 1507 Mitochondrial markers—such as citrate synthase activity as an enzymatic matrix marker—
 1508 provide a link to the tissue of origin on the basis of calculating the mitochondrial recovery,
 1509 *i.e.*, the fraction of mitochondrial marker obtained from a unit mass of tissue. Total
 1510 mitochondrial protein is frequently applied as a mitochondrial marker, which is restricted to
 1511 isolated mitochondria.

- 1512 • In studies of permeabilized cells, the viability of the cell culture or cell suspension of origin
 1513 should be reported. Normalization should be evaluated for total cell count or viable cell
 1514 count.
- 1515 • Terms and symbols are summarized in **Table 8**. Their use will facilitate transdisciplinary
 1516 communication and support further developments towards a consistent theory of
 1517 bioenergetics and mitochondrial physiology. Technical terms related to and defined with
 1518 normal words can be used as index terms in databases, support the creation of ontologies
 1519 towards semantic information processing (MitoPedia), and help in communicating analytical
 1520 findings as impactful data-driven stories. ‘*Making data available without making it*
 1521 *understandable may be worse than not making it available at all*’ (National Academies of
 1522 Sciences, Engineering, and Medicine 2018). Success will depend on taking next steps: (1)
 1523 exhaustive text-mining considering Omics data and functional data; (2) network analysis of
 1524 Omics data with bioinformatics tools; (3) cross-validation with distinct bioinformatics
 1525 approaches; (4) correlation with functional data; (5) guidelines for biological validation of
 1526 network data. This is a call to carefully contribute to FAIR principles (Findable, Accessible,
 1527 Interoperable, Reusable) for the sharing of scientific data.

1529
 1530
 1531 **Table 8. Terms, symbols, and units.**

Term	Symbol	Unit	Links and comments
1532 alternative quinol oxidase	AOX		Figure 2B
1533 amount of substance B	n_B	[mol]	
1534 ATP yield per O ₂	Y_{P_{\gg}/O_2}		P _{gg} /O ₂ ratio measured in any respiratory state
1535 catabolic reaction	k		Figure 1 and 3
1536 catabolic respiration	J_{kO_2}	varies	Figure 1 and 3
1537 cell number	N_{ce}	[x]	Table 5; $N_{ce} = N_{vce} + N_{dce}$
1538 cell respiration	J_{rO_2}	varies	Figure 1
1539 cell viability index	VI		$VI = N_{vce}/N_{ce} = 1 - N_{dce}/N_{ce}$
1540 Complexes I to IV	CI to CIV		respiratory ET Complexes; Figure 2B
1541 concentration of substance B	$c_B = n_B \cdot V^{-1}$; [B]	[mol·m ⁻³]	Box 2
1542 dead cell number	N_{dce}	[x]	Table 5; non-viable cells, loss of plasma membrane barrier function
1543 electric format	e	[C]	Table 6
1544 electron transfer system	ETS		Figure 2B, Figure 5; state
1545 flow, for substance B	I_B	[mol·s ⁻¹]	system-related extensive quantity; Figure 7
1546 flux, for substance B	J_B	varies	size-specific quantity; Figure 7
1547 inorganic phosphate	P _i		Figure 3
1548 intact cell number, viable cell number	N_{vce}	[x]	Table 5; viable cells, intact of plasma membrane barrier function
1549 LEAK	LEAK		Table 1, Figure 5; state
1550 mass format	m	[kg]	Table 4, Figure 7
1551 mass of sample X	m_X	[kg]	Table 4
1552 mass of entity X	M_X	[kg]	mass of object X; Table 4
1553 MITOCARTA			https://www.broadinstitute.org/scientific-community/science/programs/metabolic-disease-program/publications/mitocarta/mitocarta-in-0
1554 MitoPedia			http://www.bioblast.at/index.php/MitoPedia
1555 mitochondria or mitochondrial	mt		Box 1
1556 mitochondrial DNA	mtDNA		Box 1
1557 mitochondrial concentration	$C_{mtE} = mtE \cdot V^{-1}$	[mtEU·m ⁻³]	Table 4

1571	mitochondrial content	$mtE_X = mtE \cdot N_X^{-1}$	[mtEU·x ⁻¹]	Table 4
1572	mitochondrial elementary component	mtE	[mtEU]	Table 4, quantity of mt-marker
1573	mitochondrial elementary unit	mtEU	<i>varies</i>	Table 4, specific units for mt-marker
1574	mitochondrial inner membrane	mtIM		Figure 2; MIM is widely used; the first M is replaced by mt; Box 1
1575				
1576	mitochondrial outer membrane	mtOM		Figure 2; MOM is widely used; the first M is replaced by mt; Box 1
1577				
1578	mitochondrial recovery	Y_{mtE}		fraction of mtE recovered in sample from the tissue of origin
1579				
1580	mitochondrial yield	$Y_{mtE/\underline{m}}$		mt-yield per tissues mass; $Y_{mtE/\underline{m}} = Y_{mtE} \cdot D_{mtE}$
1581				
1582	molar format	\underline{n}	[mol]	Table 6
1583	negative	neg		Figure 3
1584	number concentration of X	C_{NX}	[x·m ⁻³]	Table 4
1585	number format	\underline{N}	[x]	Table 4, Figure 7
1586	number of entities X	N_X	[x]	Table 4, Figure 7
1587	number of entity B	N_B	[x]	Table 4
1588	oxidative phosphorylation	OXPPOS		Table 1, Figure 5; state
1589	oxygen concentration	$c_{O_2} = n_{O_2} \cdot V^{-1}$; [O ₂]	[mol·m ⁻³]	Section 3.2
1590	oxygen flux, in reaction r	J_{rO_2}	<i>varies</i>	Figure 1
1591	permeabilized cell number	N_{pcc}	[x]	Table 5; experimental permeabilization of plasma membrane; $N_{pcc} = N_{cc}$
1592				
1593	phosphorylation of ADP to ATP	P»		Section 2.2
1594	positive	pos		Figure 3
1595	proton in the negative compartment	H ⁺ _{neg}		Figure 3
1596	proton in the positive compartment	H ⁺ _{pos}		Figure 3
1597	rate of electron transfer in ET state	E		ET-capacity; Table 1
1598	rate of LEAK respiration	L		Table 1
1599	rate of oxidative phosphorylation	P		OXPPOS capacity; Table 1
1600	rate of residual oxygen consumption	Rox		Table 1, Figure 1
1601	residual oxygen consumption	ROX		Table 1; state
1602	respiratory supercomplex	SC I _n III _n IV _n		Box 1; supramolecular assemblies composed of variable copy numbers (n) of CI, CIII and CIV
1603				
1604				
1605	specific mitochondrial density	$D_{mtE} = mtE \cdot m_X^{-1}$	[mtEU·kg ⁻¹]	Table 4
1606	volume	V	[m ⁻³]	Table 7
1607	volume format	\underline{V}	[m ⁻³]	Table 6
1608	weight, dry weight	W_d	[kg]	used as mass of sample X ; Figure 7
1609	weight, wet weight	W_w	[kg]	used as mass of sample X ; Figure 7
1610				

1611

1612 Acknowledgements

1613 We thank M. Beno for management assistance. This publication is based upon work from
 1614 COST Action CA15203 MitoEAGLE, supported by COST (European Cooperation in Science
 1615 and Technology), and K-Regio project MitoFit (E.G.).

1616

1617 **Competing financial interests:** E.G. is founder and CEO of Oroboros Instruments, Innsbruck,
 1618 Austria.

1619

1620 References

1621

1622 Altmann R (1894) Die Elementarorganismen und ihre Beziehungen zu den Zellen. Zweite vermehrte Auflage.
 1623 Verlag Von Veit & Comp, Leipzig:160 pp.

1624 Baggeto LG, Testa-Perussini R (1990) Role of acetoin on the regulation of intermediate metabolism of Ehrlich
 1625 ascites tumor mitochondria: its contribution to membrane cholesterol enrichment modifying passive proton
 1626 permeability. Arch Biochem Biophys 283:341-8.

1627 Beard DA (2005) A biophysical model of the mitochondrial respiratory system and oxidative phosphorylation.
 1628 PLoS Comput Biol 1(4):e36.

1629 Benda C (1898) Weitere Mitteilungen über die Mitochondria. Verh Dtsch Physiol Ges:376-83.

- 1630 Birkedal R, Laasmaa M, Vendelin M (2014) The location of energetic compartments affects energetic
1631 communication in cardiomyocytes. *Front Physiol* 5:376.
- 1632 Blier PU, Dufresne F, Burton RS (2001) Natural selection and the evolution of mtDNA-encoded peptides:
1633 evidence for intergenomic co-adaptation. *Trends Genet* 17:400-6.
- 1634 Blier PU, Guderley HE (1993) Mitochondrial activity in rainbow trout red muscle: the effect of temperature on
1635 the ADP-dependence of ATP synthesis. *J Exp Biol* 176:145-58.
- 1636 Breton S, Beaupré HD, Stewart DT, Hoeh WR, Blier PU (2007) The unusual system of doubly uniparental
1637 inheritance of mtDNA: isn't one enough? *Trends Genet* 23:465-74.
- 1638 Brown GC (1992) Control of respiration and ATP synthesis in mammalian mitochondria and cells. *Biochem J*
1639 284:1-13.
- 1640 Calvo SE, Klauser CR, Mootha VK (2016) MitoCarta2.0: an updated inventory of mammalian mitochondrial
1641 proteins. *Nucleic Acids Research* 44:D1251-7.
- 1642 Calvo SE, Julien O, Clauser KR, Shen H, Kamer KJ, Wells JA, Mootha VK (2017) Comparative analysis of
1643 mitochondrial N-termini from mouse, human, and yeast. *Mol Cell Proteomics* 16:512-23.
- 1644 Campos JC, Queliconi BB, Bozi LHM, Bechara LRG, Dourado PMM, Andres AM, Jannig PR, Gomes KMS,
1645 Zambelli VO, Rocha-Resende C, Guatimosim S, Brum PC, Mochly-Rosen D, Gottlieb RA, Kowaltowski AJ,
1646 Ferreira JCB (2017) Exercise reestablishes autophagic flux and mitochondrial quality control in heart failure.
1647 *Autophagy* 13:1304-317.
- 1648 Canton M, Luvisetto S, Schmehl I, Azzone GF (1995) The nature of mitochondrial respiration and
1649 discrimination between membrane and pump properties. *Biochem J* 310:477-81.
- 1650 Carrico C, Meyer JG, He W, Gibson BW, Verdin E (2018) The mitochondrial acylome emerges: proteomics,
1651 regulation by Sirtuins, and metabolic and disease implications. *Cell Metab* 27:497-512.
- 1652 Chan DC (2006) Mitochondria: dynamic organelles in disease, aging, and development. *Cell* 125:1241-52.
- 1653 Chance B, Williams GR (1955a) Respiratory enzymes in oxidative phosphorylation. I. Kinetics of oxygen
1654 utilization. *J Biol Chem* 217:383-93.
- 1655 Chance B, Williams GR (1955b) Respiratory enzymes in oxidative phosphorylation: III. The steady state. *J Biol*
1656 *Chem* 217:409-27.
- 1657 Chance B, Williams GR (1955c) Respiratory enzymes in oxidative phosphorylation. IV. The respiratory chain. *J*
1658 *Biol Chem* 217:429-38.
- 1659 Chance B, Williams GR (1956) The respiratory chain and oxidative phosphorylation. *Adv Enzymol Relat Subj*
1660 *Biochem* 17:65-134.
- 1661 Chowdhury SK, Djordjevic J, Albensi B, Fernyhough P (2015) Simultaneous evaluation of substrate-dependent
1662 oxygen consumption rates and mitochondrial membrane potential by TMRM and safranin in cortical
1663 mitochondria. *Biosci Rep* 36:e00286.
- 1664 Cobb LJ, Lee C, Xiao J, Yen K, Wong RG, Nakamura HK, Mehta HH, Gao Q, Ashur C, Huffman DM, Wan J,
1665 Muzumdar R, Barzilai N, Cohen P (2016) Naturally occurring mitochondrial-derived peptides are age-
1666 dependent regulators of apoptosis, insulin sensitivity, and inflammatory markers. *Aging (Albany NY)* 8:796-
1667 809.
- 1668 Cohen ER, Cvitas T, Frey JG, Holmström B, Kuchitsu K, Marquardt R, Mills I, Pavese F, Quack M, Stohner J,
1669 Strauss HL, Takami M, Thor HL (2008) Quantities, units and symbols in physical chemistry, IUPAC Green
1670 Book, 3rd Edition, 2nd Printing, IUPAC & RSC Publishing, Cambridge.
- 1671 Cooper H, Hedges LV, Valentine JC, eds (2009) The handbook of research synthesis and meta-analysis. Russell
1672 Sage Foundation.
- 1673 Coopersmith J (2010) Energy, the subtle concept. The discovery of Feynman's blocks from Leibnitz to Einstein.
1674 Oxford University Press:400 pp.
- 1675 Cummins J (1998) Mitochondrial DNA in mammalian reproduction. *Rev Reprod* 3:172-82.
- 1676 Dai Q, Shah AA, Garde RV, Yonish BA, Zhang L, Medvitz NA, Miller SE, Hansen EL, Dunn CN, Price TM
1677 (2013) A truncated progesterone receptor (PR-M) localizes to the mitochondrion and controls cellular
1678 respiration. *Mol Endocrinol* 27:741-53.
- 1679 Daum B, Walter A, Horst A, Osiewacz HD, Kühlbrandt W (2013) Age-dependent dissociation of ATP synthase
1680 dimers and loss of inner-membrane cristae in mitochondria. *Proc Natl Acad Sci U S A* 110:15301-6.
- 1681 Divakaruni AS, Brand MD (2011) The regulation and physiology of mitochondrial proton leak. *Physiology*
1682 (Bethesda) 26:192-205.
- 1683 Doerrier C, Garcia-Souza LF, Krumschnabel G, Wohlfarter Y, Mészáros AT, Gnaiger E (2018) High-Resolution
1684 FluoRespirometry and OXPHOS protocols for human cells, permeabilized fibres from small biopsies of
1685 muscle, and isolated mitochondria. *Methods Mol Biol* 1782 (Palmeira CM, Moreno AJ, eds): Mitochondrial
1686 Bioenergetics, 978-1-4939-7830-4.
- 1687 Doskey CM, van 't Erve TJ, Wagner BA, Buettner GR (2015) Moles of a substance per cell is a highly
1688 informative dosing metric in cell culture. *PLOS ONE* 10:e0132572.
- 1689 Drahota Z, Milerová M, Stieglarová A, Houstek J, Ostádal B (2004) Developmental changes of cytochrome *c*
1690 oxidase and citrate synthase in rat heart homogenate. *Physiol Res* 53:119-22.

- 1691 Duarte FV, Palmeira CM, Rolo AP (2014) The role of microRNAs in mitochondria: small players acting wide.
1692 Genes (Basel) 5:865-86.
- 1693 Ehinger JK, Morota S, Hansson MJ, Paul G, Elmér E (2015) Mitochondrial dysfunction in blood cells from
1694 amyotrophic lateral sclerosis patients. *J Neurol* 262:1493-503.
- 1695 Ernster L, Schatz G (1981) Mitochondria: a historical review. *J Cell Biol* 91:227s-55s.
- 1696 Estabrook RW (1967) Mitochondrial respiratory control and the polarographic measurement of ADP:O ratios.
1697 *Methods Enzymol* 10:41-7.
- 1698 Faber C, Zhu ZJ, Castellino S, Wagner DS, Brown RH, Peterson RA, Gates L, Barton J, Bickett M, Hagerty L,
1699 Kimbrough C, Sola M, Bailey D, Jordan H, Elangbam CS (2014) Cardiolipin profiles as a potential
1700 biomarker of mitochondrial health in diet-induced obese mice subjected to exercise, diet-restriction and
1701 ephedrine treatment. *J Appl Toxicol* 34:1122-9.
- 1702 Fell D (1997) Understanding the control of metabolism. Portland Press.
- 1703 Forstner H, Gnaiger E (1983) Calculation of equilibrium oxygen concentration. In: Polarographic Oxygen
1704 Sensors. Aquatic and Physiological Applications. Gnaiger E, Forstner H (eds), Springer, Berlin, Heidelberg,
1705 New York:321-33.
- 1706 Garlid KD, Beavis AD, Ratkje SK (1989) On the nature of ion leaks in energy-transducing membranes. *Biochim*
1707 *Biophys Acta* 976:109-20.
- 1708 Garlid KD, Semrad C, Zinchenko V. Does redox slip contribute significantly to mitochondrial respiration? In:
1709 Schuster S, Rigoulet M, Ouhabi R, Mazat J-P, eds (1993) Modern trends in biothermokinetics. Plenum Press,
1710 New York, London:287-93.
- 1711 Gerö D, Szabo C (2016) Glucocorticoids suppress mitochondrial oxidant production via upregulation of
1712 uncoupling protein 2 in hyperglycemic endothelial cells. *PLoS One* 11:e0154813.
- 1713 Gnaiger E. Efficiency and power strategies under hypoxia. Is low efficiency at high glycolytic ATP production a
1714 paradox? In: Surviving Hypoxia: Mechanisms of Control and Adaptation. Hochachka PW, Lutz PL, Sick T,
1715 Rosenthal M, Van den Thillart G, eds (1993a) CRC Press, Boca Raton, Ann Arbor, London, Tokyo:77-109.
- 1716 Gnaiger E (1993b) Nonequilibrium thermodynamics of energy transformations. *Pure Appl Chem* 65:1983-2002.
- 1717 Gnaiger E (2001) Bioenergetics at low oxygen: dependence of respiration and phosphorylation on oxygen and
1718 adenosine diphosphate supply. *Respir Physiol* 128:277-97.
- 1719 Gnaiger E (2009) Capacity of oxidative phosphorylation in human skeletal muscle. New perspectives of
1720 mitochondrial physiology. *Int J Biochem Cell Biol* 41:1837-45.
- 1721 Gnaiger E (2014) Mitochondrial pathways and respiratory control. An introduction to OXPHOS analysis. 4th ed.
1722 *Mitochondr Physiol Network* 19.12. Oroboros MiPNet Publications, Innsbruck:80 pp.
- 1723 Gnaiger E, Méndez G, Hand SC (2000) High phosphorylation efficiency and depression of uncoupled respiration
1724 in mitochondria under hypoxia. *Proc Natl Acad Sci USA* 97:11080-5.
- 1725 Greggio C, Jha P, Kulkarni SS, Lagarrigue S, Brosiere NT, Boutant M, Wang X, Conde Alonso S, Ofori E,
1726 Auwerx J, Cantó C, Amati F (2017) Enhanced respiratory chain supercomplex formation in response to
1727 exercise in human skeletal muscle. *Cell Metab* 25:301-11.
- 1728 Hinkle PC (2005) P/O ratios of mitochondrial oxidative phosphorylation. *Biochim Biophys Acta* 1706:1-11.
- 1729 Hofstadter DR (1979) Gödel, Escher, Bach: An eternal golden braid. A metaphorical fugue on minds and
1730 machines in the spirit of Lewis Carroll. Harvester Press:499 pp.
- 1731 Illaste A, Laasmaa M, Peterson P, Vendelin M (2012) Analysis of molecular movement reveals latticelike
1732 obstructions to diffusion in heart muscle cells. *Biophys J* 102:739-48.
- 1733 Jasienski M, Bazzaz FA (1999) The fallacy of ratios and the testability of models in biology. *Oikos* 84:321-26.
- 1734 Jepihhina N, Beraud N, Sepp M, Birkedal R, Vendelin M (2011) Permeabilized rat cardiomyocyte response
1735 demonstrates intracellular origin of diffusion obstacles. *Biophys J* 101:2112-21.
- 1736 Klepinin A, Ounpuu L, Guzun R, Chekulayev V, Timohhina N, Tepp K, Shevchuk I, Schlattner U, Kaambre T
1737 (2016) Simple oxygraphic analysis for the presence of adenylate kinase 1 and 2 in normal and tumor cells. *J*
1738 *Bioenerg Biomembr* 48:531-48.
- 1739 Klingenberg M (2017) UCP1 - A sophisticated energy valve. *Biochimie* 134:19-27.
- 1740 Koit A, Shevchuk I, Ounpuu L, Klepinin A, Chekulayev V, Timohhina N, Tepp K, Puurand M, Truu L, Heck K,
1741 Valvere V, Guzun R, Kaambre T (2017) Mitochondrial respiration in human colorectal and breast cancer
1742 clinical material is regulated differently. *Oxid Med Cell Longev* 1372640.
- 1743 Komlódi T, Tretter L (2017) Methylene blue stimulates substrate-level phosphorylation catalysed by succinyl-
1744 CoA ligase in the citric acid cycle. *Neuropharmacology* 123:287-98.
- 1745 Korn E (1969) Cell membranes: structure and synthesis. *Annu Rev Biochem* 38:263-88.
- 1746 Lane N (2005) Power, sex, suicide: mitochondria and the meaning of life. Oxford University Press:354 pp.
- 1747 Larsen S, Nielsen J, Neigaard Nielsen C, Nielsen LB, Wibrand F, Stride N, Schroder HD, Boushel RC, Helge
1748 JW, Dela F, Hey-Mogensen M (2012) Biomarkers of mitochondrial content in skeletal muscle of healthy
1749 young human subjects. *J Physiol* 590:3349-60.
- 1750 Lee C, Zeng J, Drew BG, Sallam T, Martin-Montalvo A, Wan J, Kim SJ, Mehta H, Hevener AL, de Cabo R,
1751 Cohen P (2015) The mitochondrial-derived peptide MOTS-c promotes metabolic homeostasis and reduces
1752 obesity and insulin resistance. *Cell Metab* 21:443-54.

- 1753 Lee SR, Kim HK, Song IS, Youm J, Dizon LA, Jeong SH, Ko TH, Heo HJ, Ko KS, Rhee BD, Kim N, Han J
1754 (2013) Glucocorticoids and their receptors: insights into specific roles in mitochondria. *Prog Biophys Mol*
1755 *Biol* 112:44-54.
- 1756 Leek BT, Mudaliar SR, Henry R, Mathieu-Costello O, Richardson RS (2001) Effect of acute exercise on citrate
1757 synthase activity in untrained and trained human skeletal muscle. *Am J Physiol Regul Integr Comp Physiol*
1758 280:R441-7.
- 1759 Lemieux H, Blier PU, Gnaiger E (2017) Remodeling pathway control of mitochondrial respiratory capacity by
1760 temperature in mouse heart: electron flow through the Q-junction in permeabilized fibers. *Sci Rep* 7:2840.
- 1761 Lenaz G, Tioli G, Falasca AI, Genova ML (2017) Respiratory supercomplexes in mitochondria. In: *Mechanisms*
1762 *of primary energy transduction in biology*. M Wikstrom (ed) Royal Society of Chemistry Publishing, London,
1763 UK:296-337.
- 1764 Liu S, Roellig DM, Guo Y, Li N, Frace MA, Tang K, Zhang L, Feng Y, Xiao L (2016) Evolution of mitosome
1765 metabolism and invasion-related proteins in *Cryptosporidium*. *BMC Genomics* 17:1006.
- 1766 Margulis L (1970) *Origin of eukaryotic cells*. New Haven: Yale University Press.
- 1767 Meinild Lundby AK, Jacobs RA, Gehrig S, de Leur J, Hauser M, Bonne TC, Flück D, Dandanell S, Kirk N,
1768 Kaech A, Ziegler U, Larsen S, Lundby C (2018) Exercise training increases skeletal muscle mitochondrial
1769 volume density by enlargement of existing mitochondria and not de novo biogenesis. *Acta Physiol* 222,
1770 e12905.
- 1771 Menshikova EV, Ritov VB, Fairfull L, Ferrell RE, Kelley DE, Goodpaster BH (2006) Effects of exercise on
1772 mitochondrial content and function in aging human skeletal muscle. *J Gerontol A Biol Sci Med Sci* 61:534-
1773 40.
- 1774 Menshikova EV, Ritov VB, Ferrell RE, Azuma K, Goodpaster BH, Kelley DE (2007) Characteristics of skeletal
1775 muscle mitochondrial biogenesis induced by moderate-intensity exercise and weight loss in obesity. *J Appl*
1776 *Physiol* (1985) 103:21-7.
- 1777 Menshikova EV, Ritov VB, Toledo FG, Ferrell RE, Goodpaster BH, Kelley DE (2005) Effects of weight loss
1778 and physical activity on skeletal muscle mitochondrial function in obesity. *Am J Physiol Endocrinol Metab*
1779 288:E818-25.
- 1780 Miller GA (1991) *The science of words*. Scientific American Library New York:276 pp.
- 1781 Mitchell P (1961) Coupling of phosphorylation to electron and hydrogen transfer by a chemi-osmotic type of
1782 mechanism. *Nature* 191:144-8.
- 1783 Mitchell P (2011) Chemiosmotic coupling in oxidative and photosynthetic phosphorylation. *Biochim Biophys*
1784 *Acta Bioenergetics* 1807:1507-38.
- 1785 Mogensen M, Sahlin K, Fernström M, Glintborg D, Vind BF, Beck-Nielsen H, Højlund K (2007) Mitochondrial
1786 respiration is decreased in skeletal muscle of patients with type 2 diabetes. *Diabetes* 56:1592-9.
- 1787 Mohr PJ, Phillips WD (2015) Dimensionless units in the SI. *Metrologia* 52:40-7.
- 1788 Moreno M, Giacco A, Di Munno C, Goglia F (2017) Direct and rapid effects of 3,5-diiodo-L-thyronine (T2).
1789 *Mol Cell Endocrinol* 7207:30092-8.
- 1790 Morrow RM, Picard M, Derbeneva O, Leipzig J, McManus MJ, Gouspillou G, Barbat-Artigas S, Dos Santos C,
1791 Hepple RT, Murdock DG, Wallace DC (2017) Mitochondrial energy deficiency leads to hyperproliferation of
1792 skeletal muscle mitochondria and enhanced insulin sensitivity. *Proc Natl Acad Sci U S A* 114:2705-10.
- 1793 Murley A, Nunnari J (2016) The emerging network of mitochondria-organelle contacts. *Mol Cell* 61:648-53.
- 1794 National Academies of Sciences, Engineering, and Medicine (2018) *International coordination for science data*
1795 *infrastructure: Proceedings of a workshop—in brief*. Washington, DC: The National Academies Press. doi:
1796 <https://doi.org/10.17226/25015>.
- 1797 Palmfeldt J, Bross P (2017) Proteomics of human mitochondria. *Mitochondrion* 33:2-14.
- 1798 Paradies G, Paradies V, De Benedictis V, Ruggiero FM, Petrosillo G (2014) Functional role of cardiolipin in
1799 mitochondrial bioenergetics. *Biochim Biophys Acta* 1837:408-17.
- 1800 Pesta D, Gnaiger E (2012) High-Resolution Respirometry. OXPHOS protocols for human cells and
1801 permeabilized fibres from small biopsies of human muscle. *Methods Mol Biol* 810:25-58.
- 1802 Pesta D, Hoppel F, Macek C, Messner H, Faulhaber M, Kobel C, Parson W, Burtcher M, Schocke M, Gnaiger
1803 E (2011) Similar qualitative and quantitative changes of mitochondrial respiration following strength and
1804 endurance training in normoxia and hypoxia in sedentary humans. *Am J Physiol Regul Integr Comp Physiol*
1805 301:R1078-87.
- 1806 Price TM, Dai Q (2015) The role of a mitochondrial progesterone receptor (PR-M) in progesterone action.
1807 *Semin Reprod Med* 33:185-94.
- 1808 Puchowicz MA, Varnes ME, Cohen BH, Friedman NR, Kerr DS, Hoppel CL (2004) Oxidative phosphorylation
1809 analysis: assessing the integrated functional activity of human skeletal muscle mitochondria – case studies.
1810 *Mitochondrion* 4:377-85. Puntschart A, Claassen H, Jostardt K, Hoppeler H, Billeter R (1995) mRNAs of
1811 enzymes involved in energy metabolism and mtDNA are increased in endurance-trained athletes. *Am J*
1812 *Physiol* 269:C619-25.
- 1813 Quiros PM, Mottis A, Auwerx J (2016) Mitonuclear communication in homeostasis and stress. *Nat Rev Mol*
1814 *Cell Biol* 17:213-26.

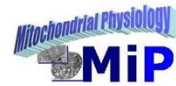
- 1815 Rackham O, Mercer TR, Filipovska A (2012) The human mitochondrial transcriptome and the RNA-binding
 1816 proteins that regulate its expression. *WIREs RNA* 3:675–95.
- 1817 Reichmann H, Hoppeler H, Mathieu-Costello O, von Bergen F, Pette D (1985) Biochemical and ultrastructural
 1818 changes of skeletal muscle mitochondria after chronic electrical stimulation in rabbits. *Pflugers Arch* 404:1-
 1819 9.
- 1820 Renner K, Amberger A, Konwalinka G, Gnaiger E (2003) Changes of mitochondrial respiration, mitochondrial
 1821 content and cell size after induction of apoptosis in leukemia cells. *Biochim Biophys Acta* 1642:115-23.
- 1822 Rice DW, Alverson AJ, Richardson AO, Young GJ, Sanchez-Puerta MV, Munzinger J, Barry K, Boore JL,
 1823 Zhang Y, dePamphilis CW, Knox EB, Palmer JD (2016) Horizontal transfer of entire genomes via
 1824 mitochondrial fusion in the angiosperm *Amborella*. *Science* 342:1468-73.
- 1825 Rich P (2003) Chemiosmotic coupling: The cost of living. *Nature* 421:583.
- 1826 Rich PR (2013) Chemiosmotic theory. *Encyclopedia Biol Chem* 1:467-72.
- 1827 Rostovtseva TK, Sheldon KL, Hassanzadeh E, Monge C, Saks V, Bezrukov SM, Sackett DL (2008) Tubulin
 1828 binding blocks mitochondrial voltage-dependent anion channel and regulates respiration. *Proc Natl Acad Sci*
 1829 *USA* 105:18746-51.
- 1830 Rustin P, Parfait B, Chretien D, Bourgeron T, Djouadi F, Bastin J, Rötig A, Munnich A (1996) Fluxes of
 1831 nicotinamide adenine dinucleotides through mitochondrial membranes in human cultured cells. *J Biol Chem*
 1832 271:14785-90.
- 1833 Saks VA, Veksler VI, Kuznetsov AV, Kay L, Sikk P, Tiivel T, Tranqui L, Olivares J, Winkler K, Wiedemann F,
 1834 Kunz WS (1998) Permeabilised cell and skinned fiber techniques in studies of mitochondrial function in
 1835 vivo. *Mol Cell Biochem* 184:81-100.
- 1836 Salabei JK, Gibb AA, Hill BG (2014) Comprehensive measurement of respiratory activity in permeabilized cells
 1837 using extracellular flux analysis. *Nat Protoc* 9:421-38.
- 1838 Sazanov LA (2015) A giant molecular proton pump: structure and mechanism of respiratory complex I. *Nat Rev*
 1839 *Mol Cell Biol* 16:375-88.
- 1840 Schneider TD (2006) Claude Shannon: biologist. The founder of information theory used biology to formulate
 1841 the channel capacity. *IEEE Eng Med Biol Mag* 25:30-3.
- 1842 Schönfeld P, Dymkowska D, Wojtczak L (2009) Acyl-CoA-induced generation of reactive oxygen species in
 1843 mitochondrial preparations is due to the presence of peroxisomes. *Free Radic Biol Med* 47:503-9.
- 1844 Schultz J, Wiesner RJ (2000) Proliferation of mitochondria in chronically stimulated rabbit skeletal muscle--
 1845 transcription of mitochondrial genes and copy number of mitochondrial DNA. *J Bioenerg Biomembr* 32:627-
 1846 34.
- 1847 Speijer D (2016) Being right on Q: shaping eukaryotic evolution. *Biochem J* 473:4103-27.
- 1848 Sugiura A, Mattie S, Prudent J, McBride HM (2017) Newly born peroxisomes are a hybrid of mitochondrial and
 1849 ER-derived pre-peroxisomes. *Nature* 542:251-4.
- 1850 Simson P, Jepihhina N, Laasmaa M, Peterson P, Birkedal R, Vendelin M (2016) Restricted ADP movement in
 1851 cardiomyocytes: Cytosolic diffusion obstacles are complemented with a small number of open mitochondrial
 1852 voltage-dependent anion channels. *J Mol Cell Cardiol* 97:197-203.
- 1853 Stucki JW, Ineichen EA (1974) Energy dissipation by calcium recycling and the efficiency of calcium transport
 1854 in rat-liver mitochondria. *Eur J Biochem* 48:365-75.
- 1855 Tonkonogi M, Harris B, Sahlin K (1997) Increased activity of citrate synthase in human skeletal muscle after a
 1856 single bout of prolonged exercise. *Acta Physiol Scand* 161:435-6.
- 1857 Torralba D, Baixauli F, Sánchez-Madrid F (2016) Mitochondria know no boundaries: mechanisms and functions
 1858 of intercellular mitochondrial transfer. *Front Cell Dev Biol* 4:107. eCollection 2016.
- 1859 Vamecq J, Schepers L, Parmentier G, Mannaerts GP (1987) Inhibition of peroxisomal fatty acyl-CoA oxidase by
 1860 antimycin A. *Biochem J* 248:603-7.
- 1861 Waczulikova I, Habodaszova D, Cagalinec M, Ferko M, Ulicna O, Mateasik A, Sikurova L, Ziegelhöffer A
 1862 (2007) Mitochondrial membrane fluidity, potential, and calcium transients in the myocardium from acute
 1863 diabetic rats. *Can J Physiol Pharmacol* 85:372-81.
- 1864 Wagner BA, Venkataraman S, Buettner GR (2011) The rate of oxygen utilization by cells. *Free Radic Biol Med*
 1865 51:700-712.
- 1866 Wang H, Hiatt WR, Barstow TJ, Brass EP (1999) Relationships between muscle mitochondrial DNA content,
 1867 mitochondrial enzyme activity and oxidative capacity in man: alterations with disease. *Eur J Appl Physiol*
 1868 *Occup Physiol* 80:22-7.
- 1869 Watt IN, Montgomery MG, Runswick MJ, Leslie AG, Walker JE (2010) Bioenergetic cost of making an
 1870 adenosine triphosphate molecule in animal mitochondria. *Proc Natl Acad Sci U S A* 107:16823-7.
- 1871 Weibel ER, Hoppeler H (2005) Exercise-induced maximal metabolic rate scales with muscle aerobic capacity. *J*
 1872 *Exp Biol* 208:1635–44.
- 1873 White DJ, Wolff JN, Pierson M, Gemmell NJ (2008) Revealing the hidden complexities of mtDNA inheritance.
 1874 *Mol Ecol* 17:4925–42.
- 1875 Wikström M, Hummer G (2012) Stoichiometry of proton translocation by respiratory complex I and its
 1876 mechanistic implications. *Proc Natl Acad Sci U S A* 109:4431-6.

1877 Williams EG, Wu Y, Jha P, Dubuis S, Blattmann P, Argmann CA, Houten SM, Amariuta T, Wolski W,
 1878 Zamboni N, Aebersold R, Auwerx J (2016) Systems proteomics of liver mitochondria function. Science 352
 1879 (6291):aad0189
 1880 Willis WT, Jackman MR, Messer JI, Kuzmiak-Glancy S, Glancy B (2016) A simple hydraulic analog model of
 1881 oxidative phosphorylation. Med Sci Sports Exerc 48:990-1000.
 1882



Mitochondrial respiratory states and rates:

Building blocks of mitochondrial physiology



Part 1 - www.mitoeagle.org/index.php/MitoEAGLE_preprint_2018-02-08

Gnaiger E^{1,2}, corresponding author
 355 co-authors, MitoEAGLE Working Group

¹Medical University Innsbruck
²Oroboros, Innsbruck, Austria

Aims

Clarity of concept and consistency of nomenclature facilitate effective transdisciplinary communication, education, and ultimately further discovery.

Adhering to uniform standards and harmonizing the terminology concerning mitochondrial respiratory states and rates will support the development of databases of mitochondrial respiratory function in cells, tissues, and species.

Summary

Recommendations on coupling control states and rates are focused on studies with mitochondrial preparations.

Fig. 1: Respiration is defined by O₂ flux balance.

Fig. 2: OXPHOS analysis is based on the study of mt- preparations. Metabolic fluxes measured in defined coupling and pathway control states provide insights into the meaning of cellular respiration.

Fig. 3: Interpretation of respiratory rates depends critically on appropriate normalization.

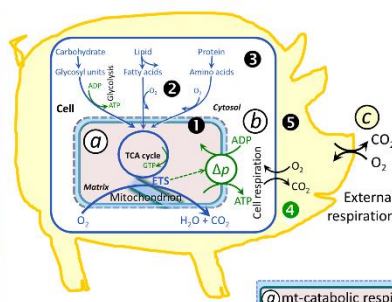
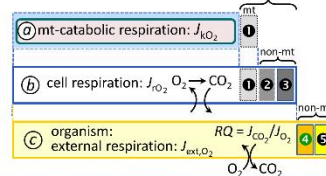


Figure 1. From mitochondrial to external respiration

Mitochondrial (mt) respiration is the oxidation of fuel substrates (electron donors) and reduction of O₂ catalysed by the electron transfer system, ETS:

- (a) mt-catabolic respiration, excluding TCA cycle, ETS;
- (b) Total cellular O₂ consumption, including mt-Rox, particularly by peroxisomal oxidases, and non-mt Rox unrelated to catabolism.
- (c) External respiration, including aerobic microbial respiration, and extracellular O₂ consumption.



MiPart by Odra Noel

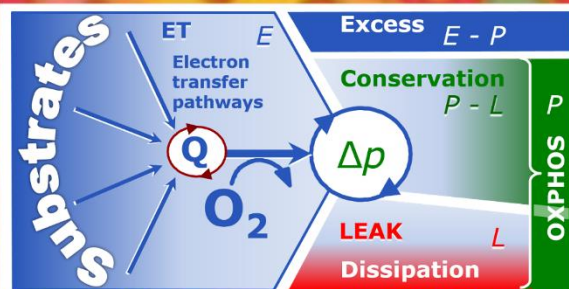


Figure 2. Respiratory states (ET, OXPHOS, LEAK) and corresponding rates (E, P, L)

Table 1. Coupling states and residual oxygen consumption in mitochondrial preparations in relation to respiration- and phosphorylation-flux, J_{kO_2} and J_{P_0} , and protonmotive force, Δp . Coupling states are established at kinetically saturating concentrations of fuel substrates and O₂.

State	J_{kO_2}	J_{P_0}	Δp	Inducing factors	Limiting factors
LEAK	L ; low, cation leak-dependent respiration	0	max.	proton leak, slip, and cation cycling	$J_{P_0} = 0$: (1) without ADP, L_S ; (2) max. ATP/ADP ratio, L_T ; or (3) inhibition of the phosphorylation-pathway, L_{Oxy}
OXPHOS	P ; high, ADP-stimulated respiration	max.	high	kinetically-saturating [ADP] and [P _i]	J_{P_0} by phosphorylation-pathway; or J_{kO_2} by ET-capacity
ET	E ; max., noncoupled respiration	0	low	optimal external uncoupler concentration for max. $J_{O_2, E}$	J_{kO_2} by ET-capacity
ROX	Rox ; min., residual O ₂ consumption	0	0	$J_{O_2, Rox}$ in non-ET-pathway oxidation reactions	inhibition of all ET-pathways; or absence of fuel substrates

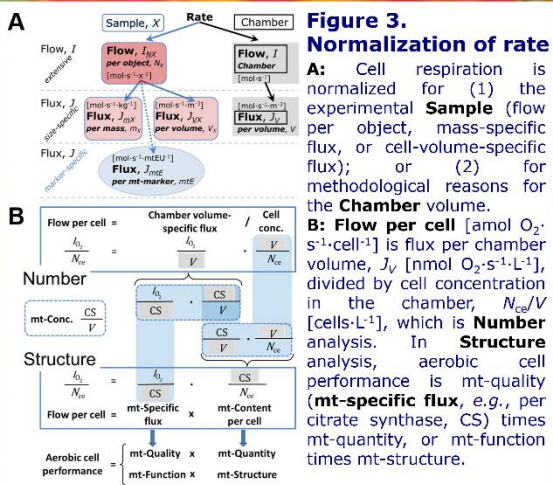


Figure 3. Normalization of rate

A: Cell respiration is normalized for (1) the experimental Sample (flow per object, mass-specific flux, or cell-volume-specific flux); or (2) for methodological reasons for the Chamber volume.

B: Flow per cell [amol O₂ s⁻¹ cell⁻¹] is flux per chamber volume, J_V [nmol O₂ s⁻¹ L⁻¹], divided by cell concentration in the chamber, N_{ce}/V [cells L⁻¹], which is **Number** analysis. In **Structure** analysis, aerobic cell performance is mt-quality (mt-specific flux, e.g., per citrate synthase, CS) times mt-quantity, or mt-function times mt-structure.